Phytochrome higher order mutants reveal a complex set of light responses in the moss *Physcomitrium patens*

Jinhong Yuan[1], Tengfei Xu[1,3], and Andreas Hiltbrunner[1,2,*]

[1] Faculty of Biology, University of Freiburg, Germany
[2] Signalling Research Centres BIOSS and CIBSS, University of Freiburg, Germany
[3] present address: State Key Laboratory of Crop Stress Biology for Arid Areas, College of Horticulture, Northwest A&F University, Yangling 712100, P.R. China

[*] Corresponding author; andreas.hiltbrunner@biologie.uni-freiburg.de; phone: +49 761 203 2709

Total word count:	6,500
Word count Introduction:	798
Word count Materials and Methods:	1,945
Word count Results:	2,055
Word count Discussion:	1,702

SUMMARY

- The colonisation of land by plants is considered a major event in the history of Earth, which ultimately also allowed animals to colonise land. The change from aquatic to terrestrial habitats brought a number of challenges for plants, including light conditions that are different on land compared to aquatic habitats.
- Phytochromes are photoreceptors enabling plants to respond to various light conditions. Independent gene duplication events resulted in small phytochrome gene families in mosses, ferns, and seed plants. This phytochrome diversity is hypothesised to be critical for sensing and adapting to different light conditions, but experimental evidence for this idea is lacking for mosses and ferns.
- The model moss species *Physcomitrium patens* contains seven phytochromes grouped into three clades. Here, we used CRISPR/Cas9 generated single and higher order mutants to investigate the role of different phytochromes in light-regulation of protonema and gametophore growth, protonema branching, and induction of gametophores.
- We found both specific and partially overlapping roles for the three clades of moss phytochromes in regulating these responses in red, far-red, or blue light, and we identified a mechanism for sensing simulated canopy shade that is different from the mechanism used by seed plants.

Keywords:
Evolution of light signalling, photomorphogenesis, *Physcomitrium patens*, phytochrome, subfunctionalisation.

INTRODUCTION

Phytochromes are photoreceptors in plants and several fungal, algal, and prokaryotic lineages. All these phytochromes share a common photosensory core module (PCM) essential for light absorption and photoconversion (Li *et al.*, 2015; Rockwell & Lagarias, 2020; Cheng *et al.*, 2021). This PCM is combined with additional lineage-specific domains. In canonical plant phytochromes, the PCM is fused to a C-terminal module consisting of two PAS domains and a histidine kinase related domain (HKRD), which however lacks histidine kinase activity. The origin of canonical plant phytochromes has been placed in a common ancestor of extant streptophytes (Li *et al.*, 2015; Wang *et al.*, 2020); for details on the evolution of canonical plant phytochromes, we refer readers to Rockwell and Lagarias (2020). Single phytochrome homologues have been found in liverworts (Marchantiophyta) and hornworts (Anthocerophyta), while independent gene duplication events resulted in small gene families in mosses, ferns, and seed plants (Li *et al.*, 2015).

By absorbing light, phytochromes reversibly convert between the inactive Pr and the active Pfr state, which have absorption peaks in red (R, 660 nm) and far-red light (FR, 720 nm), respectively. The R and FR light content in the environment therefore determines the relative level of phytochrome in the active state (Pfr/Ptot = Pfr/[Pr+Pfr]) (Legris *et al.*, 2019).

Phytochromes from seed plants cluster into three clades, *PHYA*, *PHYB/E*, and *PHYC* (Li *et al.*, 2015). PhyA and phyB are the dominant phytochromes in *Arabidopsis* and also play an important role in other seed plants for regulation of growth and development and the adaptation to changes in the environment (Franklin & Quail, 2010; Legris *et al.*, 2019). PhyA is highly abundant in etiolated seedlings and rapidly degraded when converted to Pfr, while phyB is the most abundant phytochrome in light-grown plants and much more stable than phyA (Sharrock & Clack, 2002). PhyB is active in light conditions in which Pfr/Ptot levels are high, such as R light or sunlight, whereas it is largely inactive in FR light or deep canopy shade. For reasons that are not yet well understood, phyA is physiologically active in FR light, deep canopy shade, and other conditions that result in low Pfr/Ptot levels (Legris *et al.*, 2019). Additional phytochromes present only in some taxa may further extend the range of light conditions than can be discriminated, and it has been proposed that the expansion of the phytochrome family promoted the radiation of seed plants (Mathews, 2010; Li *et al.*, 2015). It has also been observed that species-rich fern and moss lineages tend to have more phytochrome copies than species-poor lineages. This correlation may be interpreted to mean that the structural and functional diversity of phytochromes facilitates adaptation to different light conditions (Li *et al.*, 2015).

The moss *Physcomitrium patens* contains seven phytochromes, *PHY1-PHY4* and *PHY5a*, *b*, and *c*, clustering into three clades, *PHY1/3*, *PHY2/4*, and *PHY5* (Supporting Information Fig. **S1**) (Li *et al.*, 2015). In many other mosses, phytochromes are also represented by at least one *PHY1/3*, *PHY2/4*, and *PHY5* clade phytochrome (Supporting Information Fig. **S2**). Light-activated

phytochromes are transported into the nucleus in *Physcomitrium*, similar to seed plant phytochromes (Possart & Hiltbrunner, 2013), and homologues of key factors of light signalling identified in *Arabidopsis* are also present in *Physcomitrium* (e.g. PHYTOCHROME INTERACTING FACTORs [PIFs], CONSTITUTIVELY PHOTOMORPHOGENIC 1 [COP1], SUPPRESSOR OF PHYA-105 [SPAs], and ELONGATED HYPOCOTYL 5 [HY5]) (Yamawaki *et al.*, 2011; Ranjan *et al.*, 2014; Possart *et al.*, 2017; Xu & Hiltbrunner, 2017; Artz *et al.*, 2019; Cheng *et al.*, 2021). Despite these similarities, also mechanistic differences have been reported between phytochrome signalling in *Physcomitrium* and *Arabidopsis*, reflecting a common origin of components and mechanisms followed by independent evolution over more than 400 million years (Ranjan *et al.*, 2014; Possart *et al.*, 2017; Xu & Hiltbrunner, 2017; Artz *et al.*, 2019; McDaniel, 2021).

Due to the independent expansion of the phytochrome family in mosses, it is impossible to infer the specificity and function of moss phytochromes from studies on phytochromes of seed plants (Li *et al.*, 2015). Mittmann *et al.* (2004) reported that a cytosolic pool of PHY4 modulates the phototropic response of protonema filaments in red light, and Trogu *et al.* (2021) generated a phytochrome septuple mutant and a set of phytochrome higher order mutants using CRISPR/Cas9 to show that PHY5a inhibits gravitropism of red light-grown protonema filaments. However, a systematic analysis of the function and specificity of all the seven *Physcomitrium* phytochromes is still lacking. Here we used CRISPR/Cas9 to generate single and higher order phytochrome mutants in the moss *Physcomitrium patens* to identify the role of the different phytochromes in regulation of protonema and gametophore growth, protonema branching, and induction of gametophores. This approach revealed a complex pattern of light responses with both specific and partially overlapping roles for the three clades of moss phytochromes in sensing different light conditions.

MATERIAL AND METHODS

Plant materials, growth conditions, and phenotypic analysis

Physcomitrium patens strain Gransden 2004 (Rensing *et al.*, 2008) was generally cultivated on Knop's medium (Reski & Abel, 1985; Frank *et al.*, 2005) in a growth chamber at 24 ± 1 °C under a 16/8 h light/dark photoperiod with a light intensity of 50-70 µmol m^{-2} s^{-1} (Supporting Information Fig. **S3**). Unless otherwise stated, the plates were incubated horizontally (if the plates were incubated vertically, this is indicated in the figure legends).

Light conditions used for experiments were as follows. Standard growth conditions: 50 µmol m^{-2} s^{-1}, 16/8 h light/dark cycles, 24 °C; red light (R): 20 µmol m^{-2} s^{-1}, continuous light, 24 °C; far-red light (FR): 20 µmol m^{-2} s^{-1}, continuous light, 24 °C; blue light (B): 12 µmol m^{-2} s^{-1}, continuous light, 24 °C; low R:FR conditions (W+FR): 25 µmol m^{-2} s^{-1} W + 25 µmol m^{-2} s^{-1} FR, continuous light, 24 °C; high R:FR conditions (W): 25 µmol m^{-2} s^{-1} W, continuous light, 24 °C; dark (D), 24 °C. Light spectra are shown in Supporting Information Fig. **S3**.

For analysis of gametophore induction, a piece of freshly fragmented protonema tissue from a 7 day-old protonema culture grown on Knop's medium (1 % [w/v] agar) overlaid with cellophane was spotted onto Knop's medium (1 % [w/v] agar) supplemented with 0.5 % sucrose. Sixteen plants per genotype were grown on square plates (16 cm diagonal). Plates were incubated under the respective light conditions for 14 days and gametophores were then counted. Pictures were taken using a scanner (Epson Perfection V700 Photo).

For measurement of gametophore length, protonema cultures were prepared and gametophores were grown as described above for up to 45 days in the respective light conditions. Gametophores from at least five plants per genotype/condition were placed on a new plate to take pictures; length was then measured using the ImageJ software.

For analysis of protonema branching and caulonema/chloronema, protonema cultures were fragmented weekly using a T18 Ultra Turrax disperser (IKA) and spotted again onto Knop's medium (1 % [w/v] agar) overlaid with cellophane. Freshly fragmented protonema cultures were spotted onto a new plate containing Knop's medium (1 % [w/v] agar) supplemented with 0.5 % sucrose. Plates were incubated in the respective light conditions for the time indicated in the figure legends. Pictures were taken using a scanner (Epson Perfection V700 Photo) or binocular microscope (Zeiss, Axio Zoom.V16).

To analyse growth habit, a piece of freshly fragmented protonema culture was inoculated onto plates containing Knop's medium (1 % [w/v] agar) supplemented with 0.5 % sucrose and incubated in the respective light conditions for the time indicated in the figure legend. Pictures were taken using a scanner (Epson Perfection V700 Photo).

Plasmid constructs used to generate *phy* mutant lines

Single and higher order *phy* mutant lines were generated by CRISPR/Cas9 as described by Ermert *et al.* (2019) and Lopez-Obando *et al.* (2016). Higher order mutants were generated by using lower order mutants for mutagenesis or by mutating wildtype *Physcomitrium patens* (Supporting Information Fig. **S4**). Single guide RNAs (sgRNAs) were designed using the CRISPR-P 2.0 online tool (Liu *et al.*, 2017). To construct a sgRNA plasmid, a 488 bp gBlock DNA fragment containing the *PpU6* promoter and a fragment coding for the sgRNA flanked by *attB1*/*attB2* sites for Gateway cloning was synthesised at Integrated DNA Technologies (Leuven, Belgium) (Supporting Information Table **S1**). The gBlock fragments were then recombined into pDONR207-KanR by BP Gateway cloning to obtain the respective pEntPp-U6-sgRNA-KanR plasmids (Supporting Information Table **S2**). The Gateway reaction mixtures contained 3 µl of U6-sgRNA gBlock fragment (50 ng μl^{-1}), 1 µl of pDONR207-KanR (150 ng μl^{-1}), and 1 µl of BP clonase II mix (Invitrogen; Cat. No. 11789-020); they were incubated at 25 °C for 2 hours and then transformed into *E.coli*. For selection, bacteria were spread on LB plates supplemented with 10 mg l^{-1} Gentamycin (Duchefa Biochemie; Cat. No. G0124.0010). Details of plasmid constructs used in this study can be found in Supporting Information Table **S2**.

Transformation of *Physcomitrium patens*

Physcomitrium patens transformation was performed as described in Grimsley *et al.* (1977) and Schaefer *et al.* (1991) with modifications. Protoplasts were isolated from young protonema tissue cultured for 4 days at 25 °C in continuous light on cellophane sheets on Knop's medium (1 % [w/v] agar) supplemented with 5 mM ammonium tartrate. 1.2×10^6 protoplasts were transformed with a mix of the plasmid encoding Cas9 (pAct-Cas9) and one or several plasmids encoding sgRNAs (pEntPp-U6-sgRNA-KanR). Ten µg of pAct-Cas9 and a total of 10 µg of pEntPp-U6-sgRNA-KanR were used per transformation approach; for generation of higher order mutants, the respective pEntPp-U6-sgRNA-KanR plasmids were combined. After transformation, protoplasts were incubated in PRML liquid medium (10 mM $CaCl_2$ [added before use], 5 mM Diammonium tartrate; 8.5 % [w/v] D-mannitol; liquid Knop's medium to 1 l) for 24 hours in the dark and pelleted by centrifugation (60 × *g* for 10 min). Protoplasts were then resuspended in 1 ml sterile 8 % (w/v) D-mannitol, 7 ml of molten PRMT medium (10 mM $CaCl_2$ [added before use]; 5 mM Diammonium tartrate; 8 % [w/v] D-mannitol; liquid Knop's medium to 1 l; 0.4 % [w/v] Agar) were added, and resuspended protoplasts were dispensed onto three 90 mm petri dishes containing PRMB medium (10 mM $CaCl_2$ [added before use]; 5 mM Diammonium tartrate; 6 % [w/v] D-mannitol; liquid Knop's medium to 1 l; 0.7 % [w/v] Agar) overlaid with cellophane. Plates were incubated in standard growth conditions for 5 days. Regenerated protoplasts with cellophane were first transferred to Knop's medium (1 % [w/v] agar) supplemented with 5 mM ammonium tartrate and 12.5 µg ml^{-1} G418 (Duchefa Biochemie; Cat. No. G0175.0005) for another 5 days and then to normal Knop's medium (1 % [w/v] agar) supplemented with 5 mM ammonium tartrate for 7 days. Resistant plants

were then transferred to Knop's medium (1 % [w/v] agar) and grown for 2 weeks in standard growth conditions. DNA was then extracted from gametophores and mutation of the target gene(s) tested by PCR and sequencing.

DNA extraction and on-target mutation analysis

One or two gametophores from 2 to 3-week-old moss plant were transferred into 1.5 ml Eppendorf tubes containing seven glass beads per tube. Gametophores were frozen in liquid nitrogen and ground using the TissueLyser (Qiagen; Cat. No. 85220). DNA was extracted as described in Lopez-Obando *et al.* (2016). Analysis of on-target mutations was performed by PCR using 1.5 µl extracted DNA solution as a template. Primers for PCR were designed to obtain about 200 bp fragments flanking the CRISPR/Cas9 target site. PCR fragments were analysed by 3 % agarose TBE gel-electrophoresis to detect deletions or insertions; fragments from potential mutants were sequenced. Primers used for the amplification and subsequent Sanger sequencing are listed in Supporting Information Table **S3**. Mutants containing deletions and/or insertions resulting in a frameshift were selected for further research (Supporting Information Fig. **S4**).

***Physcomitrium* protein extraction and immunoblot analysis**

Freshly fragmented protonema cultures of *Physcomitrium* lines expressing YFP-tagged PHYs (Possart & Hiltbrunner, 2013) were incubated for 10 days under standard growth conditions on solid Knop's medium overlaid with a cellophane sheet. Gametophores were obtained from protonema inoculated onto solid Knop's medium. Gametophores developed after approximately 45 days incubation in standard growth conditions. For dark-adaptation of the protonema cultures and gametophores, plates were incubated in darkness for 4 days. Protonema cultures and gametophores were then exposed to red light (20 µmol m^{-2} s^{-1}) or far-red light (20 µmol m^{-2} s^{-1}) (Supporting Information Fig. **S3**), or kept in the dark and harvested into Eppendorf tubes. For protein extraction, plant material was homogenised in liquid nitrogen using glass beads and the TissueLyser (Qiagen; Cat. No. 85220). Protein extraction buffer (50 mM Tris, pH 7.5, 150 mM NaCl, 1 mM EDTA, 10 % [v/v] glycerol, 1 mM DTT, and 1 × complete Protease Inhibitor [Roche; Cat. No. 058929700001]) was added to homogenised plant material (100 µl extraction buffer per 100 mg plant material). Samples were then vortexed and centrifuged at 16,000 × *g* at 4 °C for 10 min. The supernatant was pipetted into a new tube and an equal volume of 2 × SDS-PAGE loading buffer (100 mM Tris-HCl pH 6.8, 4 % [w/v] SDS, 20 % [v/v] glycerol, 0.05 % [w/v] bromophenol blue) was added; the samples were then incubated at 95 °C for 5 min. Protein extracts were separated by SDS-PAGE and then transferred to PVDF membrane (Immobilon-P Transfer Membrane; Roth, Karlsruhe, Germany; Cat. No. T831.1) in transfer buffer (25 mM Tris, 192 mM glycine, 10 % [v/v] methanol) by applying 250 mA for 2 hours in the cold room. After blocking with 5 % (w/v) skim milk powder in PBST buffer (20 mM $NaPO_4$ pH 7.4, 150 mM NaCl,

200 0.05 % [v/v] Tween-20) for 1 hour, membranes were incubated in blocking buffer containing anti-
201 GFP antibody (Roche; Cat. No. 11814460001; Dilution: 1:1,000 diluted in PBST) or anti-Actin
202 antibody (Sigma-Aldrich; Cat. No. A0480; Dilution: 1: 5,000 diluted in PBST) for 2 hours at room
203 temperature and then washed three times with washing buffer (50 mM Tris-HCl, pH 7.5; 0.5 M
204 NaCl; 0.05 % [v/v] Tween 20). Rabbit anti-Mouse IgG (whole molecule)-Peroxidase antibody
205 (Sigma-Aldrich; Cat. No. A9044; Dilution: 1:20,000 diluted in PBST) was used as secondary
206 antibody together with the Amersham ECL Prime Western Blotting Detection Reagent (GE
207 Healthcare; Cat. No. RPN2232) for signal detection.

208 **Statistical analysis**

209 Statistical analysis was performed by one-way or two-way ANOVA followed by Tukey's HSD test as
210 indicated in the figure legends; $p < 0.05$. Plots were generated by GraphPad Prism 8 or
211 Python/Matplotlib.

212 **Phylogenetic tree**

213 *Arabidopsis thaliana* phyA and phyB protein sequences were used to search the i) nr,
214 refseq_protein, and swissprot protein databases at NCBI using BLASTP with default settings, ii)
215 the onekp/prot/v5/onek protein database at CNG using BLASTP with default settings, and iii) the
216 nt, refseq_rna, est, and tsa nucleotide databases at NCBI using TBLASTN with default settings;
217 the search was restricted to sequences from mosses (Bryophyta; NCBI taxid 3208) (Altschul *et al.*,
218 1997; NCBI Resource Coordinators, 2013; Carpenter *et al.*, 2019). The resulting dataset was then
219 filtered for full length or close to full length phytochrome sequences by requesting a minimal
220 alignment length of 1,100 amino acid residues and a minimal BLAST score of 3,000. The dataset
221 was then filtered to remove identical or highly similar sequences originating from the same species;
222 identical/highly similar sequences from different species were retained. To this end, sequences
223 were sorted into species-specific subsets containing all sequences from one species. Within each
224 species-specific subset, all sequences were compared to each other by pairwise alignment;
225 sequences with a score/sequence length value > 0.97 were classified as identical/highly similar
226 and only the longer sequence was retained. All species-specific subsets were then merged again
227 into a single dataset (Supporting Information Data **S1**) and a sequence alignment was performed
228 using ClustalΩ with default settings (Sievers *et al.*, 2011). The sequence alignment was then
229 curated by Gblock using the following parameters: minimum number of sequences for a conserved
230 position: 46, minimum number of sequences for a flanking position: 77, maximum number of
231 contiguous nonconserved positions: 8, minimum length of a block: 10, allowed gap positions: none,
232 use similarity matrices: yes (Castresana, 2000) (Supporting Information Data **S1**). The curated
233 alignment was then submitted to PhyML online (http://www.atgc-montpellier.fr/phyml/) to calculate
234 a maximum-likelihood tree; default settings were used except for "Branch Supports" for which

"Standard bootstrap analysis" with 100 repeats was selected (Guindon & Gascuel, 2003) (Supporting Information Data **S1**). The resulting tree was then processed using the online tool iTOL v5 (https://itol.embl.de/) (Letunic & Bork, 2021); branches with bootstrap support < 50/100 were deleted.

Accession numbers

Accession numbers of genes/proteins used in this study are listed in Supporting Information Table **S4**.

RESULTS

The *phy12345abc* septuple mutant is impaired in growth and development

To analyse the function of phytochromes in the moss model species *Physcomitrium patens*, we generated single and higher order phytochrome loss-of-function mutants using CRISPR/Cas9 (Supporting Information Fig. **S4**) (Lopez-Obando *et al.*, 2016). The *phy1 phy2 phy3 phy4 phy5a phy5b phy5c* septuple mutant, referred to as *phy12345abc*, does not contain any functional phytochromes. When grown in white or blue light, the number of gametophores was reduced in the *phy12345abc* mutant compared to the wildtype (Fig. **1a**, Supporting Information Fig. **S5a, b**). In addition, filaments of the *phy12345abc* mutant grown in white light were brownish, which is different from the green protonema filaments observed for the wildtype (Supporting Information Fig. **S5a**). In red and far-red light, the *phy12345abc* mutant was unable to induce gametophores and only few protonema filaments emerged from cultures inoculated onto agar plates (Fig. **1a**, Supporting Information Fig. **S5c**). In contrast, wildtype plants grown in red and white light were similar, and also formed few elongated gametophores in far-red light. We conclude that phytochromes are necessary to control growth and development of *Physcomitrium* in response to red, far-red, blue, and white light.

PHY5a/b/c are the primary phytochromes for responses to red light

To investigate potential subfunctionalisation among PHY1/3, PHY2/4, and PHY5 clade phytochromes, we generated *phy13*, *phy24*, and *phy5abc* mutants (Supporting Information Fig. **S4**) (Lopez-Obando *et al.*, 2016). After growth in white or red light for two weeks, wildtype, *phy13*, and *phy24* plants were similar, while the *phy5abc* triple mutant was different (Fig. **1b**). In particular in red light, the *phy5abc* mutant had more caulonema filaments than the wildtype, but formed fewer side branches (Fig. **1b,** Supporting Information Fig. **S6**). In addition, induction of gametophores was almost fully abolished in *phy5abc* grown in red light, and the number of gametophores was also reduced in white light (Fig. **1b**, Supporting Information Fig. **S7**). Gametophores of *phy5abc* were similar in length to those of the wildtype when grown in white light, but considerably longer in red light (Supporting Information Fig. **S7**). In contrast to *phy5abc*, red light-grown *phy24* and *phy1234* mutant plants had shorter gametophores than the wildtype, but otherwise were similar to wildtype plants when cultivated in white or red light (Fig. **1b,** Supporting Information Fig. **S7, S8**).

We also generated mutants deficient in all phytochromes except those from one clade to investigate if phytochromes of the respective clade are sufficient for specific light responses (Supporting Information Fig. **S4**) (Lopez-Obando *et al.*, 2016). Apart from gametophore length in red light, the *phy1234* mutant is very similar to the wildtype when grown in white or red light, suggesting PHY5 clade phytochromes are the primary red light receptors (Supporting Information Fig. **S9**). In contrast, the *phy245abc* mutant is severely impaired in growth and development in

white and in particular in red light, similar to the *phy12345abc* septuple mutant. Thus, PHY1/3 clade phytochromes cannot sustain basal development in red light. Finally, the *phy135abc* mutant forms few gametophores in red light, indicating that PHY2/4 clade phytochromes contribute to responses in red light, but to a lesser extent than PHY5 clade phytochromes.

PHY5a plays a dominant role in the red light response

To investigate potential redundancy among the three PHY5 clade phytochromes, we generated single and double mutants and cultivated them in red light (Supporting Information Fig. **S4**) (Lopez-Obando *et al.*, 2016). The *phy5a*, *phy5ab*, and *phy5ac* mutants formed fewer but longer gametophores than the wildtype, but we did not find obvious differences between the wildtype and the other mutants (Fig. **2**). White light-grown *phy5a*, *phy5ab*, and *phy5ac* mutants also tended to have less but slightly longer gametophores than the wildtype (Supporting Information Fig. **S10**). These results indicate that PHY5a plays a dominant role in the induction of gametophores and inhibition of gametophore growth in red light. To validate the importance of PHY5a in red light responses, we examined the phenotype of the *phy12345bc* sextuple mutant which only contains PHY5a as functional phytochrome (Supporting Information Fig. **S4, S11**). The *phy12345bc* mutant was still able to induce gametophores in red light, further confirming the dominant role of PHY5a in red light perception. However, *phy5ab* and *phy5ac* mutants still induce more gametophores than *phy5abc* when grown in white light (Supporting Information Fig. **S10a**), and *phy5ab* also has more gametophores than *phy5abc* in red light (Fig. **2c**), showing that PHY5b and PHY5c contribute to a low extent to induction of gametophores in white and red light.

PHY4 is the dominant phytochrome promoting gametophore growth in red light

PHY2/4 are partially redundant with PHY5a/b/c regarding the induction of gametophores in red light (Supporting Information Fig. **S9**), while PHY2/4 and PHY5a/b/c have opposite effects on the growth of gametophores (Supporting Information Fig. **S7**). To test if there is redundancy between PHY2 and PHY4, we tested the phenotype of *phy2* and *phy4* single mutants (Supporting Information Fig. **S4**) (Lopez-Obando *et al.*, 2016). The number of gametophores in red light-grown wildtype, *phy2*, and *phy4* plants was similar, while growth of gametophores was reduced in the *phy4* but not the *phy2* mutant compared to the wildtype (Fig. **3**). We did not observe obvious differences between the wildtype and *phy2* or *phy4* grown in white light (Supporting Information Fig. **S12**). This indicates that PHY4 promotes gametophore growth in red light.

PHY1/3 clade phytochromes are far-red light receptors

We have previously shown that levels of endogenous PHY1 and PHY3 tagged with YFP are reduced in plants exposed to red light (Possart & Hiltbrunner, 2013) but did not investigate if this is a specific property of PHY1/3 clade phytochromes. To address this question, we used a set of

Physcomitrium lines containing the coding sequence of YFP fused to the 3' end of the coding sequence of endogenous *PHY1*, *PHY2*, *PHY3*, *PHY4*, or *PHY5a* for immunoblot analysis (Possart & Hiltbrunner, 2013). Levels of PHY1-YFP and PHY3-YFP in gametophore and protonema cultures were not affected by far-red light, but were downregulated after 1 hour exposure to red light and barely detectable after 6 hours (Supporting Information Fig. **S13a, c, f, h**). In contrast, PHY2-YFP, PHY4-YFP, and PHY5a-YFP levels in cultures exposed to red light were similar to levels in far-red light and the dark control (Supporting Information Fig. **S13b, d, e, g, i, j**). The rapid downregulation of PHY1-YFP and PHY3-YFP levels in red light is reminiscent of the regulation of phyA in seed plants, which is much more abundant in etiolated seedlings than upon exposure to red or white light (Sharrock & Clack, 2002; Legris *et al.*, 2019). In contrast, this difference is much less prominent for phyB (Sharrock & Clack, 2002).

Even though PHY1/3 clade phytochromes are more closely related to PHY2/4 and PHY5 clade phytochromes from mosses than to seed plant phyA (Li *et al.*, 2015), we hypothesised that PHY1/3 could play a role as far-red light receptors similar to phyA. When grown in far-red light, *phy13* exhibited reduced branching of protonema filaments compared to the wildtype and failed to induce gametophores, whereas there were no obvious differences between the wildtype and the *phy24* and *phy5abc* mutants (Fig. **4a, b**, Supporting Information Fig. **S14a**). After four months, however, the *phy13* mutant formed few small gametophores in far-red light in contrast to the *phy1234* mutant (Supporting Information Fig. **S14b**), indicating a minor contribution of PHY2/4 to this response that is masked in presence of functional PHY1/3. In agreement with this, *phy245abc* quintuple mutants were still able to induce gametophores in far-red light, but to a lesser extent than the wildtype, while *phy135abc* and *phy1234* did not induce gametophores in far-red light (Supporting Information Fig. **S15**).

To investigate if PHY2/4 and in particular PHY1/3 also play a role in regulation of growth of gametophores in far-red light, we induced gametophores in *phy13*, *phy24*, and *phy1234* by cultivation in white light for 10 days and then transferred the plants to far-red light. Gametophores of wildtype, *phy24*, and *phy13* plants strongly elongated in far-red light, although growth appeared to be delayed in *phy13* compared to *phy24* and the wildtype (Fig. **4c**, Supporting Information Fig. **S16**). In contrast, the *phy1234* quadruple mutant did not respond to far-red light with increased gametophore growth, even not after 3 months (Supporting Information Fig. **S17**). We conclude that PHY1/3 play a role as far-red light receptors and that under specific conditions also PHY2/4 can promote a response to far-red light.

PHY1 is active in the absence of other phytochromes and induces gametophores in far-red light

Using CRISPR/Cas9, we also generated *phy1* and *phy3* single mutants as well as *phy124* and *phy234* triple mutants (Supporting Information Fig. **S4**) (Lopez-Obando *et al.*, 2016). In contrast to

347 the mutants deficient in both PHY1/3 clade phytochromes, the single and triple mutants containing
348 either functional PHY1 or PHY3 still induced gametophores in far-red light (Supporting Information
349 Fig. **S18**). Due to the low number of gametophores induced in far-red light, we could not reliably
350 quantify potential differences in gametophore growth between wildtype, *phy124*, and *phy234*
351 plants, but when visually inspected, *phy124* gametophores often appeared slightly shorter and less
352 well developed than *phy234* gametophores. Despite the uncertainty of this observation, we
353 generated the *phy2345abc* sextuple mutant to test if PHY1, the PHY1/3 clade phytochrome still
354 present in *phy234*, would be active even in the absence of any other functional phytochrome
355 (Supporting Information Fig. **S4**) (Lopez-Obando *et al.*, 2016). When grown in white light,
356 *phy2345abc* formed only very few and tiny gametophores, and in red light, induction of
357 gametophores was fully abolished (Supporting Information Fig. **S11**), suggesting PHY1 is
358 physiologically inactive in red light. In contrast, the *phy2345abc* sextuple mutant grown in far-red
359 light was able to form gametophores (Supporting Information Fig. **S11**).

360 ***Physcomitrium* phytochromes are required for responding to blue light**

361 Phytochromes are most known as sensors for the red to far-red light range of the light spectrum.
362 However, induction of gametophores in the *phy12345abc* septuple mutant was largely abolished in
363 blue light, and also the *phy5abc* triple mutant was affected in gametophore induction under these
364 conditions, indicating PHY5a/b/c play a role in the response to blue light (Fig. **1a,** Supporting
365 Information Fig. **S19**). In addition, we found that after 45 days of growth in blue light, the *phy1234*
366 quadruple mutant showed strongly elongated gametophores compared to the wildtype, while we
367 did not observe this phenotype for *phy1*, *phy2*, *phy3* and *phy4* single or *phy13* and *phy24* double
368 mutants (Fig. **5**). This is not due to generally increased growth in *phy1234* since in other light
369 conditions, the *phy1234* mutant had even shorter gametophores than the wildtype (Fig. **4, 6,**
370 Supporting Information Fig. **S8, S16, S17**). Furthermore, compared to the wildtype, we observed
371 reduced protonema growth in blue light for *phy1234* and to a lesser extent for *phy5abc* (Supporting
372 Information Fig. **S19**).

373 ***Physcomitrium* responds to low R:FR light depending on phytochromes**

374 A low red:far-red light (R:FR) ratio in the environment is an important warning signal of canopy
375 shade and competition. In shade-intolerant seed plants, low R:FR light triggers a suite of
376 responses collectively referred to as the shade avoidance syndrome (SAS). Enhanced growth is
377 part of the SAS and serves to outcompete neighbouring plants and secure access to sunlight
378 (Franklin & Quail, 2010; Fiorucci & Fankhauser, 2017). As comparably small plants, mosses will
379 not be able to compete with much larger vascular plants. However, even in a small-scale
380 environment, sensing neighbouring (moss) plants and being able to adjust growth accordingly
381 could be beneficial. *Physcomitrium* wildtype plants grown in white light supplemented with far-red

light showed elongated gametophores compared to plants grown in white light (Fig. **6**), confirming that also *Physcomitrium* is able to sense and respond to such light conditions. The *phy5abc* mutant, which is deficient in the primary red light sensing phytochromes, had longer gametophores than wildtype plants when grown in white light, but further enhanced growth of gametophores when exposed to white light supplemented with far-red light. Thus, *phy5abc* is still able to distinguish between high and low R:FR light conditions. Gametophore growth in *phy13* and *phy24* double mutants was very similar to the wildtype both in white light and white light supplemented with far-red light; however, enhanced growth in response to supplemented far-red light was fully abolished in the *phy1234* quadruple mutant (Fig. **6,** Supporting Information Fig. **S20**). We conclude that PHY1/3 and PHY2/4 clade phytochromes act redundantly to distinguish between high and low R:FR conditions and promote gametophore growth in low R:FR light.

DISCUSSION

Research over the last three decades has shown that gene duplication events and subfunctionalisation resulted in phytochromes with different specificities in seed plants (Legris *et al.*, 2019), but this has not been investigated for mosses and ferns in which phytochromes are also represented by small gene families similar to seed plants (Li *et al.*, 2015). Using CRISPR/Cas9-generated single and higher order phytochrome mutants in the moss *Physcomitrium patens*, we now have shown that PHY5 clade phytochromes are the primary red light receptors, while PHY1/3 clade phytochromes are involved in responses to far-red light, similar to phyA in seed plants (Supporting Information Fig. **S21**). Except for promoting gametophore growth in red light, we did not find any responses that depend specifically on PHY2/4 clade phytochromes, but PHY2/4 clade phytochromes appear to act in part redundantly with PHY1/3 clade phytochromes in responses to low R:FR and blue light and with PHY5 clade phytochromes in responses to red light.

Based on different higher order phytochrome mutants, Trogu *et al.* (2021) concluded that PHY5a inhibits gravitropism of protonema filaments in red light. Here, we investigated other physiological responses, such as protonema growth and branching, ratio between caulonema and chloronema, or induction and growth of gametophores, in mutants deficient in phytochromes of specific clades. We found that PHY5 clade phytochromes play a general role as red light receptors and affect all these responses. Comparison of single, double, and triple mutants of PHY5 clade phytochromes suggest a dominant role of PHY5a, which is supported by the finding that sextuple mutants containing PHY5a as the only functional phytochrome look similar to wildtype plants, except that they are slightly dwarfed. Only in the absence of other functional PHY5 clade phytochromes, a positive effect of PHY5b and PHY5c on the induction of gametophores in white light (and to a lesser degree in red light) is visible. RNA-seq expression data for PHY5 clade phytochromes from PEATmoss show that *PHY5a* expression is generally higher than expression of *PHY5c*, but lower than expression of *PHY5b* (Supporting Information Fig. **S22**) (Fernandez-Pozo *et al.*, 2020). Thus, there is no direct correlation between transcript level and physiological effect of PHY5a, PHY5b, and PHY5c, indicating that protein abundance or activity may be regulated or that PHY5a, PHY5b, and PHY5c differ with regard to their capacity to trigger downstream signalling.

We have previously shown that far-red light promotes spore germination and growth of protonema and gametophores, but the photoreceptor mediating these responses remained elusive (Possart & Hiltbrunner, 2013). Here, we found that mutants lacking functional PHY1/3 clade phytochromes are unable to induce gametophores in far-red light and also show reduced branching of protonema filaments, while gametophore growth is only slightly affected. PHY1/3 clade phytochromes hence play an essential role as far-red light receptors in regulation of protonema branching and gametophore induction, while gametophore growth in far-red light is redundantly regulated by PHY1/3 clade phytochromes and other phytochromes. In contrast to

429 PHY5 clade phytochromes, among which PHY5a plays a dominant role, we found that PHY1 and
430 PHY3 are largely redundant. The quintuple mutant containing PHY1 and PHY3 as the only
431 functional phytochromes looks very similar to the phytochrome septuple mutant when grown in red
432 or white light, suggesting PHY1/3 clade phytochromes are barely physiologically active under
433 these conditions.

434 In contrast to PHY1/3 and PHY5 clade phytochromes, PHY2/4 clade phytochromes
435 contribute to red and far-red light induced responses and often act redundantly with PHY1/3 or
436 PHY5 clade phytochromes. A notable exception is gametophore growth in red light, which is
437 promoted by PHY2/4 clade phytochromes but inhibited by PHY5 clade phytochromes. Analysis of
438 *phy2* and *phy4* single mutants suggest a dominant role of PHY4 in promoting gametophore growth
439 in red light. PHY2 appears to be less abundant in protonema than PHY4, but we did not detect
440 such a clear difference in gametophores, suggesting that the different effect of PHY2 and PHY4 on
441 growth of gametophores can hardly be explained by different protein abundance.

442 Although land plant phytochromes are most known for their function as red and far-red light
443 receptors, they also absorb in the blue light range of the light spectrum. Blue light yields > 40 %
444 Pfr/Ptot at photoequilibrium (Mancinelli, 1994), and several responses to blue light in Arabidopsis
445 have been reported to depend on phytochromes (Lariguet & Fankhauser, 2004; Castillon *et al.*,
446 2009; Jia *et al.*, 2022). Here, we found that the *Physcomitrium* phytochrome septuple mutant is
447 affected in normal growth and development also when cultivated in blue light. The *phy5abc* mutant
448 is impaired in induction of gametophores in blue light and to a minor degree in protonema growth.
449 Growth of protonema is even more reduced in *phy1234*, while gametophore growth is enhanced in
450 the absence of functional PHY1/3 and PHY2/4 clade phytochromes. Thus, it is clear that
451 phytochromes are required for responding to blue light, but we cannot rule out the possibility that
452 they contribute to blue light responses in a light-independent manner by acting downstream of
453 dedicated blue light receptors, such as cryptochromes or phototropins (Imaizumi *et al.*, 2002;
454 Kasahara *et al.*, 2004). However, this does not affect the conclusion that phytochromes in
455 *Physcomitrium* are essential for proper responding to blue light.

456 Sensing the R:FR ratio is a fundamental function of phytochromes (Mathews, 2006). A low
457 R:FR ratio is a hallmark of canopy shade and an early warning signal of competition. In shade-
458 intolerant seed plants such as Arabidopsis, low R:FR light leads to a change in resource allocation
459 allowing the plant to promote growth and thus escape from shade (Franklin & Whitelam, 2005;
460 Legris *et al.*, 2019). Low R:FR conditions trigger this response by inactivation of phyB, while it is
461 inhibited by activation of phyB in sunlight, where the R:FR ratio is high. We found that low R:FR
462 light promotes growth of gametophores in *Physcomitrium*, and in previous reports it has been
463 shown that also other non-seed plants are able to sense the R:FR ratio (Mathews, 2006). This
464 response was fully abolished in *phy1234*, while *phy5abc* still was able to increase growth of
465 gametophores in low R:FR light. Thus, in contrast to the growth response in seed plants in low

466 R:FR conditions, gametophore growth in low R:FR light in *Physcomitrium* appears to depend on
467 the activation of the far-red light sensing PHY1/3 and PHY2/4 clade phytochromes rather than on
468 the inactivation of the red light sensing PHY5 clade phytochromes. Although it is clear that
469 *Physcomitrium* can sense and respond to low R:FR light conditions, it remains to be investigated if
470 enhanced growth of gametophores in low R:FR light indeed is an adaptation to canopy shade or
471 competition by neighbours that increases fitness under these conditions. Given the small size of
472 moss plants, it appears unlikely that increased growth in shade conditions will allow them to
473 compete with much larger (vascular) plants, but it still could be an advantage when competing for
474 light with other moss plants. However, it should be kept in mind that factors other than shade
475 conditions also can affect the R:FR ratio. Water vapour, for instance, increases the R:FR ratio
476 because humid air is absorbing much stronger in the far-red than red light range of the light
477 spectrum (Doroszewski *et al.*, 2015; Kotilainen *et al.*, 2020). Therefore, it has been speculated that
478 phytochromes also might play a role as sensors of atmospheric humidity (Doroszewski *et al.*,
479 2015). So we cannot rule out the possibility that *Physcomitrium* (also) uses the R:FR ratio to sense
480 environmental cues other than canopy shade.

481 It is intriguing that responses to far-red light in *Physcomitrium* require continuous irradiation
482 and depend on a homologue of seed plant FAR-RED ELONGATED HYPOCOTYL 1 (FHY1)/FHY1-
483 LIKE (FHL), and that the abundance of the primary far-red light sensing phytochromes, PHY1 and
484 PHY3, is downregulated in red light (Possart & Hiltbrunner, 2013). These are also hallmarks of the
485 far-red high irradiance response (HIR) and phyA in seed plants. We therefore speculate that key
486 components that determine the action spectra of phyA and PHY1/3 clade phytochromes might be
487 similar despite the independent evolution of phyA and PHY1/3 from a phytochrome in a common
488 ancestor of seed plants and mosses. This hypothesis also raises the question of whether these
489 components then would be the result of convergent evolution in seed plants and mosses or
490 whether they would have been already present in a common ancestor.

491 We have identified the specific phytochromes required to control physiological responses,
492 such as protonema branching or induction and growth of gametophores, in different light
493 conditions. However, how signals from different phytochromes – and potentially other
494 photoreceptors, such as cryptochromes (Imaizumi *et al.*, 2002) – are integrated, is still unknown.
495 For instance, PHY1/2/3/4 promote gametophore growth in low R:FR light and red light, while they
496 have little effect in white light, but inhibit growth of gametophores in blue light; PHY5a/b/c have an
497 opposite effect compared to PHY1/2/3/4 in red light and further add to the complexity in regulation
498 of gametophore growth. Differential activation or inhibition of downstream signalling components
499 by different phytochromes could play a role in this complex regulatory network. Furthermore,
500 heterodimerisation between different phytochromes, as observed in Arabidopsis (Sharrock &
501 Clack, 2004), may result in phytochrome heterodimers with unique function and specificity and may
502 also contribute to signal integration. Finally, identification of potential phytochrome downstream

503 signalling factors in *Physcomitrium* so far relied on searching for homologues of factors involved in
504 light signalling in seed plants (Yamawaki *et al.*, 2011; Possart & Hiltbrunner, 2013; Ranjan *et al.*,
505 2014; Possart *et al.*, 2017; Artz *et al.*, 2019), but an unbiased approach that could identify light
506 signalling components unique to *Physcomitrium* (or mosses in general) is still lacking. Given that
507 mosses and seed plants have evolved independently for more than 400 million years (Frangedakis
508 *et al.*, 2021), such factors may well exist.

509 Overall, characterisation of CRISPR/Cas9-generated phytochrome higher order mutants
510 revealed a complex set of light responses in the moss *Physcomitrium patens*. We have shown that
511 independent gene duplication events in mosses resulted in phytochromes that regulate responses
512 in different light conditions, including not only red and far-red light, but also blue light and light
513 conditions that simulate canopy shade. This supports the idea that expansion of the phytochrome
514 gene family followed by subfunctionalisation could be an important mechanism to facilitate the
515 adaptation of plants to diverse light conditions.

ACKNOWLEDGEMENTS

This project was carried out in the framework of MAdLand (https://madland.science, DFG priority programme 2237) and AH is grateful for funding by the DFG (HI 1369/8-1, Project ID 440515704). This study was also supported by the German Research Foundation (DFG) under Germany's Excellence Strategy (EXC-2189 – Project ID 390939984) and PhD fellowships from the Chinese Science Council (CSC) to TX and JY (CSC number: 201706760057). We thank Prof. Fabien Nogué (INRA Centre de Versailles-Grignon, IJPB (UMR1318), Versailles Cedex, France) for kindly providing the pDONR207 and pAct-Cas9 plasmids and for technical advice on applying the CRISPR/Cas9 system in *Physcomitrium patens*.

AUTHOR CONTRIBUTIONS

Conceptualisation: JY, AH. Investigation: JY, TX. Visualisation: JY. Writing – original draft: JY, AH. Writing – review and editing: JY, TX, AH. Project administration: AH; Funding acquisition: JY, TX, AH.

DATA AVAILABILITY

The data supporting the findings of this study can be found in the article or in the accompanying Supporting Information.

532 **REFERENCES**

Altschul SF, Madden TL, Schäffer AA, Zhang J, Zhang Z, Miller W, Lipman DJ. **1997**. Gapped BLAST and PSI-BLAST: a new generation of protein database search programs. *Nucleic Acids Research* **25**: 3389–3402.

Artz O, Dickopf S, Ranjan A, Kreiss M, Abraham ET, Boll V, Rensing SA, Hoecker U. **2019**. Characterization of *spa* mutants in the moss *Physcomitrella* provides evidence for functional divergence of *SPA* genes during the evolution of land plants. *New Phytologist* **224**: 1613–1626.

Carpenter EJ, Matasci N, Ayyampalayam S, Wu S, Sun J, Yu J, Jimenez Vieira FR, Bowler C, Dorrell RG, Gitzendanner MA, *et al.* 2019. Access to RNA-sequencing data from 1,173 plant species: The 1000 Plant transcriptomes initiative (1KP). *GigaScience* **8**: giz126.

Castillon A, Shen H, Huq E. **2009**. Blue light induces degradation of the negative regulator phytochrome interacting factor 1 to promote photomorphogenic development of Arabidopsis seedlings. *Genetics* **182**: 161–171.

Castresana J. **2000**. Selection of conserved blocks from multiple alignments for their use in phylogenetic analysis. *Molecular Biology and Evolution* **17**: 540–552.

Cheng M-C, Kathare PK, Paik I, Huq E. **2021**. Phytochrome signaling networks. *Annual Review of Plant Biology* **72**: 217–244.

Doroszewski A, Górski T, Kozyra J. **2015**. Atmospheric moisture controls far-red irradiation: a probable impact on the phytochrome. *International Agrophysics* **29**: 283–289.

Ermert AL, Nogué F, Stahl F, Gans T, Hughes J. **2019**. CRISPR/Cas9-mediated knockout of *Physcomitrella patens* phytochromes. *Methods in Molecular Biology (Clifton, N.J.)* **2026**: 237–263.

Fernandez-Pozo N, Haas FB, Meyberg R, Ullrich KK, Hiss M, Perroud P-F, Hanke S, Kratz V, Powell AF, Vesty EF, *et al.* 2020. PEATmoss (Physcomitrella Expression Atlas Tool): a unified gene expression atlas for the model plant *Physcomitrella patens*. *Plant Journal* **102**: 165–177.

Fiorucci A-S, Fankhauser C. **2017**. Plant strategies for enhancing access to sunlight. *Current Biology* **27**: R931–R940.

Frangedakis E, Shimamura M, Villarreal JC, Li F-W, Tomaselli M, Waller M, Sakakibara K, Renzaglia KS, Szövényi P. **2021**. The hornworts: morphology, evolution and development. *New Phytologist* **229**: 735–754.

Frank W, Decker EL, Reski R. **2005**. Molecular tools to study *Physcomitrella patens*. *Plant Biology (Stuttgart, Germany)* **7**: 220–227.

Franklin KA, Quail PH. **2010**. Phytochrome functions in *Arabidopsis* development. *Journal of Experimental Botany* **61**: 11–24.

Franklin KA, Whitelam GC. **2005**. Phytochromes and shade-avoidance responses in plants. *Annals of Botany* **96**: 169–175.

Grimsley NH, Ashton NW, Cove DJ. **1977**. The production of somatic hybrids by protoplast fusion in the moss, *Physcomitrella patens*. *Molecular & General Genetics* **154**: 97–100.

Guindon S, Gascuel O. **2003**. A simple, fast, and accurate algorithm to estimate large phylogenies by maximum likelihood. *Systematic Biology* **52**: 696–704.

Imaizumi T, Kadota A, Hasebe M, Wada M. **2002**. Cryptochrome light signals control development to suppress auxin sensitivity in the moss *Physcomitrella patens*. *Plant Cell* **14**: 373–386.

Jia X, Song M, Wang S, Liu T, Wang L, Guo L, Su L, Shi Y, Zheng X, Yang J. **2022**. Arabidopsis phytochromes A and B synergistically repress SPA1 under blue light. *Journal of Integrative Plant Biology*: jipb.13412.

Kasahara M, Kagawa T, Sato Y, Kiyosue T, Wada M. **2004**. Phototropins mediate blue and red light-induced chloroplast movements in *Physcomitrella patens*. *Plant Physiology* **135**: 1388–1397.

Kotilainen T, Aphalo Pj, Brelsford Cc, Böök H, Devraj S, Heikkilä A, Hernández R, Kylling A, Lindfors Av, Robson Tm. **2020**. Patterns in the spectral composition of sunlight and biologically meaningful spectral photon ratios as affected by atmospheric factors. *Agricultural and Forest Meteorology* **291**: 108041.

Lariguet P, Fankhauser C. **2004**. Hypocotyl growth orientation in blue light is determined by phytochrome A inhibition of gravitropism and phototropin promotion of phototropism. *Plant J.* **40**: 826–834.

Legris M, Ince YÇ, Fankhauser C. **2019**. Molecular mechanisms underlying phytochrome-controlled morphogenesis in plants. *Nature Communications* **10**: 5219.

Letunic I, Bork P. **2021**. Interactive Tree Of Life (iTOL) v5: an online tool for phylogenetic tree display and annotation. *Nucleic Acids Research* **49**: W293–W296.

Li F-W, Melkonian M, Rothfels CJ, Villarreal JC, Stevenson DW, Graham SW, Wong GK-S, Pryer KM, Mathews S. **2015**. Phytochrome diversity in green plants and the origin of canonical plant phytochromes. *Nature Communications* **6**: 7852.

Liu H, Ding Y, Zhou Y, Jin W, Xie K, Chen L-L. **2017**. CRISPR-P 2.0: An improved CRISPR-Cas9 tool for genome editing in plants. *Molecular Plant* **10**: 530–532.

Lopez-Obando M, Hoffmann B, Géry C, Guyon-Debast A, Téoulé E, Rameau C, Bonhomme S, Nogué F. **2016**. Simple and efficient targeting of multiple genes through CRISPR-Cas9 in *Physcomitrella patens*. *Genes, Genomes, Genetics* **6**: 3647–3653.

Mancinelli AL. **1994**. The physiology of phytochrome action. In: Kendrick RE, Kronenberg GHM, eds. Photomorphogenesis in Plants. Dordrecht: Kluwer Academic Publishers, 211–269.

Mathews S. **2006**. Phytochrome-mediated development in land plants: Red light sensing evolves to meet the challenges of changing light environments. *Molecular Ecology* **15**: 3483–3503.

Mathews S. **2010**. Evolutionary studies illuminate the structural-functional model of plant phytochromes. *Plant Cell* **22**: 4–16.

McDaniel SF. **2021**. Bryophytes are not early diverging land plants. *New Phytologist* **230**: 1300–1304.

Mittmann F, Brücker G, Zeidler M, Repp A, Abts T, Hartmann E, Hughes J. **2004**. Targeted knockout in *Physcomitrella* reveals direct actions of phytochrome in the cytoplasm. *Proceedings of the National Academy of Sciences of the United States of America* **101**: 13939–13944.

NCBI Resource Coordinators. **2013**. Database resources of the National Center for Biotechnology Information. *Nucleic Acids Research* **41**: D8–D20.

Possart A, Hiltbrunner A. **2013**. An evolutionarily conserved signaling mechanism mediates far-red light responses in land plants. *Plant Cell* **25**: 102–114.

Possart A, Xu T, Paik I, Hanke S, Keim S, Hermann H-M, Wolf L, Hiß M, Becker C, Huq E, *et al.* 2017. Characterization of phytochrome interacting factors from the moss *Physcomitrella patens* illustrates conservation of phytochrome signaling modules in land plants. *Plant Cell* **29**: 310–330.

Ranjan A, Dickopf S, Ullrich KK, Rensing SA, Hoecker U. **2014**. Functional analysis of COP1 and SPA orthologs from *Physcomitrella* and rice during photomorphogenesis of transgenic *Arabidopsis* reveals distinct evolutionary conservation. *BMC Plant Biology* **14**: 178.

Rensing SA, Lang D, Zimmer AD, Terry A, Salamov A, Shapiro H, Nishiyama T, Perroud P-F, Lindquist EA, Kamisugi Y, *et al.* 2008. The *Physcomitrella* genome reveals evolutionary insights into the conquest of land by plants. *Science* **319**: 64–69.

Reski R, Abel WO. **1985**. Induction of budding on chloronemata and caulonemata of the moss, *Physcomitrella patens*, using isopentenyladenine. *Planta* **165**: 354–358.

Rockwell NC, Lagarias JC. **2020**. Phytochrome evolution in 3D: deletion, duplication, and diversification. *New Phytologist* **225**: 2283–2300.

Schaefer D, Zryd J-P, Knight CD, Cove DJ. **1991**. Stable transformation of the moss *Physcomitrella patens*. *Molecular & General Genetics* **226**: 418–424.

Sharrock RA, Clack T. **2002**. Patterns of expression and normalized levels of the five *Arabidopsis* phytochromes. *Plant Physiology* **130**: 442–456.

Sharrock RA, Clack T. **2004**. Heterodimerization of type II phytochromes in Arabidopsis. *Proceedings of the National Academy of Sciences of the United States of America* **101**: 11500–11505.

Sievers F, Wilm A, Dineen D, Gibson TJ, Karplus K, Li W, Lopez R, McWilliam H, Remmert M, Söding J, *et al.* 2011. Fast, scalable generation of high-quality protein multiple sequence alignments using Clustal Omega. *Molecular Systems Biology* **7**: 539.

Trogu S, Ermert AL, Stahl F, Nogué F, Gans T, Hughes J. **2021**. Multiplex CRISPR-Cas9 mutagenesis of the phytochrome gene family in *Physcomitrium (Physcomitrella) patens*. *Plant Molecular Biology* **107**: 327–336.

Wang S, Li L, Li H, Sahu SK, Wang H, Xu Y, Xian W, Song B, Liang H, Cheng S, *et al.* 2020. Genomes of early-diverging streptophyte algae shed light on plant terrestrialization. *Nature Plants* **6**: 95–106.

Xu T, Hiltbrunner A. **2017**. PHYTOCHROME INTERACTING FACTORs from *Physcomitrella patens* are active in *Arabidopsis* and complement the *pif* quadruple mutant. *Plant Signaling and Behavior* **12**: e1388975.

Yamawaki S, Yamashino T, Nakanishi H, Mizuno T. **2011**. Functional characterization of *HY5* homolog genes involved in early light-signaling in *Physcomitrella patens*. *Bioscience, Biotechnology, and Biochemistry* **75**: 1533–1539.

533 **SUPPORTING INFORMATION**

534 **Fig. S1** Maximum Likelihood was used to infer the phylogenetic tree of moss phytochromes.
535 **Fig. S2** PHY1/3, PHY2/4, and PHY5 clade phytochromes in mosses.
536 **Fig. S3** Spectra for light sources used in this study.
537 **Fig. S4** CRISPR/Cas9-generated mutations in phytochrome genes.
538 **Fig. S5** Magnifications of pictures shown in Fig. 1a.
539 **Fig. S6** Protonema growth and branching of the *phy5abc* triple mutant in red light.
540 **Fig. S7** Quantification of gametophore number and length of WT and mutant plants grown in
541 white or red light.
542 **Fig. S8** Induction and growth of gametophores of *phy1234* in white and red light.
543 **Fig. S9** Phytochrome higher order mutants grown in red or white light.
544 **Fig. S10** Induction and growth of gametophores in mutants deficient in PHY5 clade
545 phytochromes exposed to white light.
546 **Fig. S11** PHY5a and PHY1 are sufficient for gametophore induction in red and far-red light,
547 respectively.
548 **Fig. S12** Gametophore number and length of *phy2* and *phy4* single mutants grown in white
549 light.
550 **Fig. S13** Phytochrome protein levels in *Physcomitrium* exposed to red or far-red light.
551 **Fig. S14** The *phy13* mutant is affected in protonema branching and gametophore induction in
552 far-red light.
553 **Fig. S15** PHY1/3 clade phytochromes are required for induction of gametophores in far-red
554 light.
555 **Fig. S16** The *phy1234* mutant is impaired in gametophore growth in far-red light.
556 **Fig. S17** Gametophore growth of WT and *phy1234* mutant plants in far-red light.
557 **Fig. S18** PHY1 and PHY3 induce gametophores in far-red light.
558 **Fig. S19** *phy1234* and *phy5abc* grown in blue light.
559 **Fig. S20** Enhanced gametophore growth in low R:FR light is impaired in *phy1234*.
560 **Fig. S21** *Physcomitrium* phytochromes respond to diverse light conditions and play specific and
561 overlapping roles in sensing different light qualities.
562 **Fig. S22** Tissue-specificity and light-regulation of expression of *Physcomitrium* phytochromes.
563 **Table S1** gBlock fragments containing the U6 promoter and coding for the respective sgRNAs
564 used in this study.
565 **Table S2** Cloning of plasmid constructs and references to plasmids used in this study.
566 **Table S3** Primers used for characterisation of *phy* mutant lines by PCR and sequencing.
567 **Table S4** Accession numbers of genes/proteins used in this study.

Data S1 Phytochrome sequences, aligned sequences, curated sequences, and tree file for Supporting Information Fig. S1 and S2.

570 **FIGURES**

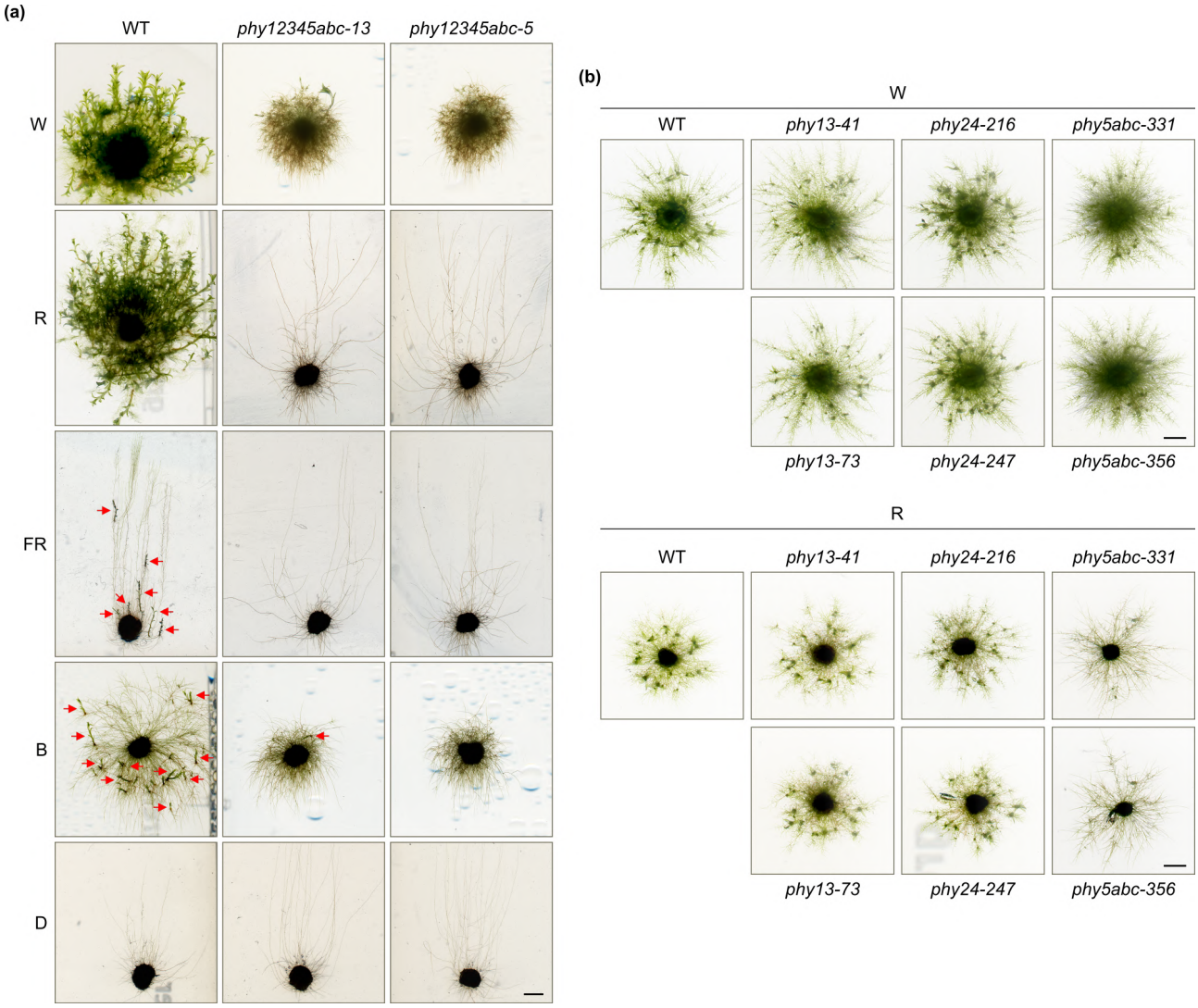

571 **Fig. 1** Effects of multiple phytochrome gene mutations on growth and development of
572 *Physcomitrium*. (a) Representative pictures of wildtype (WT) and two independent *phy12345abc*
573 septuple mutant lines grown in different light conditions. Freshly fragmented WT and *phy12345abc*
574 protonema cultures were spotted onto solid Knop's medium supplemented with 0.5 % sucrose.
575 Plates were incubated vertically in standard growth conditions (white light, W, 50 µmol m^{-2} s^{-1}), red
576 light (R, 20 µmol m^{-2} s^{-1}), far-red light (FR, 20 µmol m^{-2} s^{-1}), blue light (B, 12 µmol m^{-2} s^{-1}), or dark
577 conditions (D) for 45 days. Scale bar = 2 mm; magnifications are shown in Supporting Information
578 Fig. **S5**. (b) Representative pictures of WT, and two independent *phy13*, *phy24*, and *phy5abc*
579 mutant lines grown in W (50 µmol m^{-2} s^{-1}) or R (20 µmol m^{-2} s^{-1}) for 14 days. Scale bar = 2 mm.
580 Quantification of gametophore number per plant and gametophore length is shown in Supporting
581 Information Fig. **S7**.

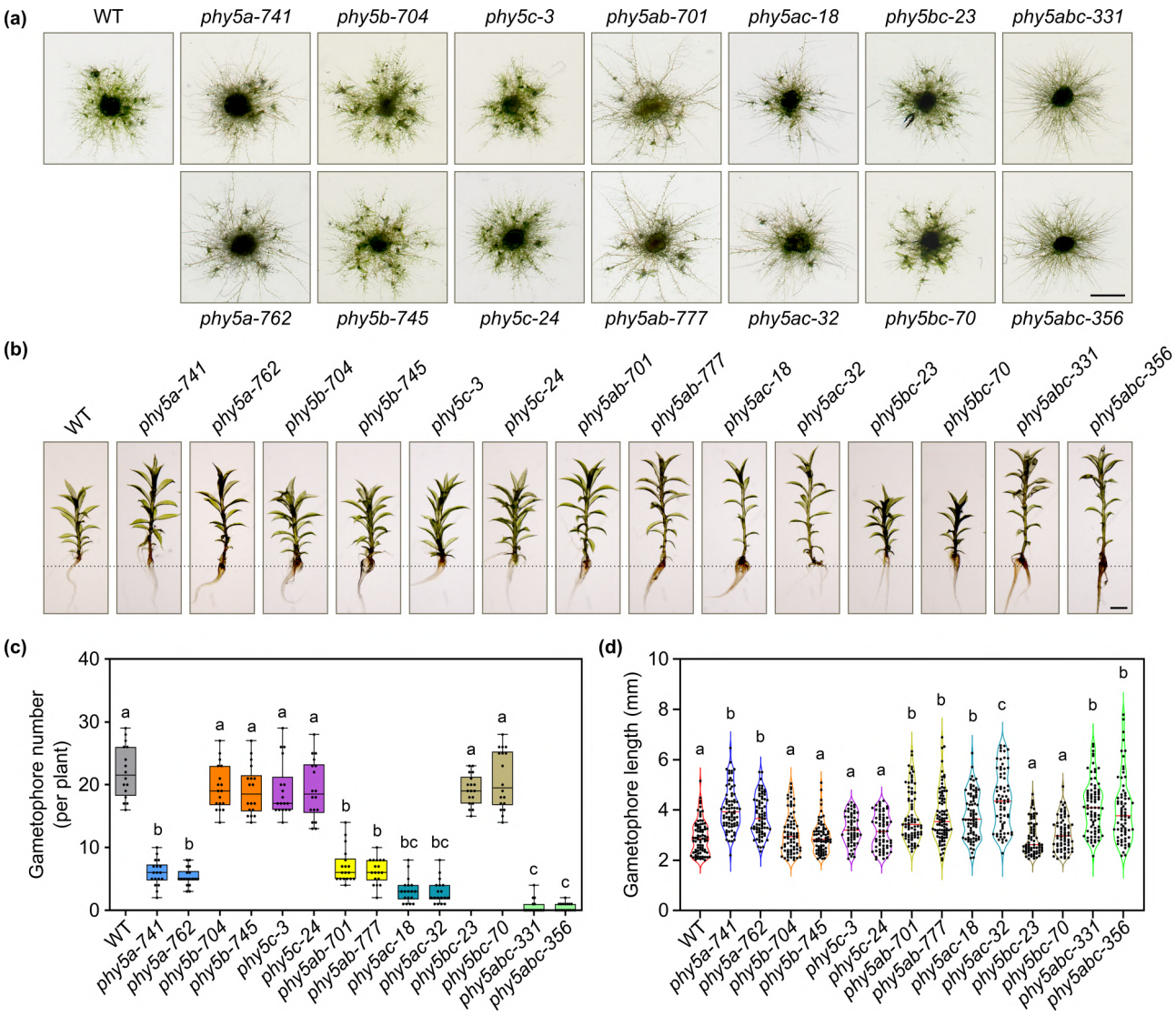

Fig. 2 PHY5a controls the induction and growth of gametophores in red light. (a) Representative pictures of WT, *phy5a*, *phy5b*, *phy5c*, *phy5ab*, *phy5ac*, *phy5bc*, and *phy5abc* plants (two independent lines for each mutant) grown in red light (R, 20 μmol m^{-2} s^{-1}) for 14 days. Scale bar = 2 mm. (b) Representative pictures of gametophores of WT and mutant plants grown in R (20 μmol m^{-2} s^{-1}) for 45 days. Scale bar = 1 mm. (c) Gametophores were counted for WT and mutant plants grown in red light (R, 20 μmol m^{-2} s^{-1}) for 14 days. Data are shown as box plot (number of plants ≥ 16); different letters indicate significant differences as determined by one-way ANOVA followed by post-hoc Tukey's HSD test; $p < 0.05$. (d) Length of gametophores was measured for WT and mutant plants grown in red light (R, 20 μmol m^{-2} s^{-1}) for 45 days. The length of > 60 gametophores was measured. Data are shown as violin plot; different letters indicate significant differences as determined by one-way ANOVA followed by post-hoc Tukey's HSD test; $p < 0.05$.

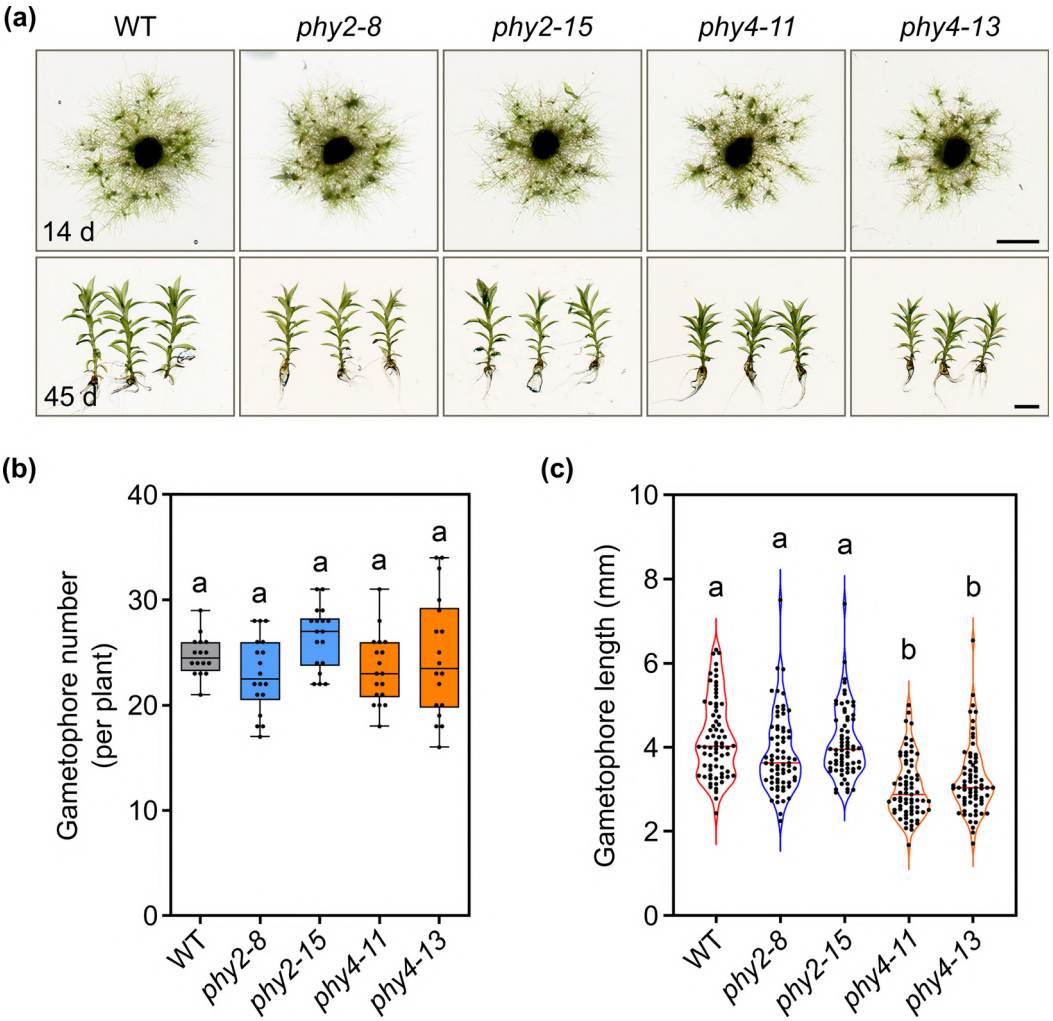

Fig. 3 The *phy4* single mutant has short gametophores in red light. (a) Representative pictures of WT, *phy2*, and *phy4* plants (two independent lines for each mutant) grown in red light (R, 20 µmol m^{-2} s^{-1}) for 14 days (upper panel). After 45 days, representative gametophores were picked from each plant (lower panel). Scale bar = 2 mm. (b) Gametophores were counted for WT and mutant plants grown in red light (R, 20 µmol m^{-2} s^{-1}) for 14 days. Data are shown as box plot (number of plants ≥ 16); different letters indicate significant differences as determined by one-way ANOVA followed by post-hoc Tukey's HSD test; $p < 0.05$. (c) Length of gametophores was measured for WT and mutant plants grown in red light (R, 20 µmol m^{-2} s^{-1}) for 45 days. The length of > 60 gametophores was measured. Data are shown as violin plot; different letters indicate significant differences as determined by one-way ANOVA followed by post-hoc Tukey's HSD test; $p < 0.05$.

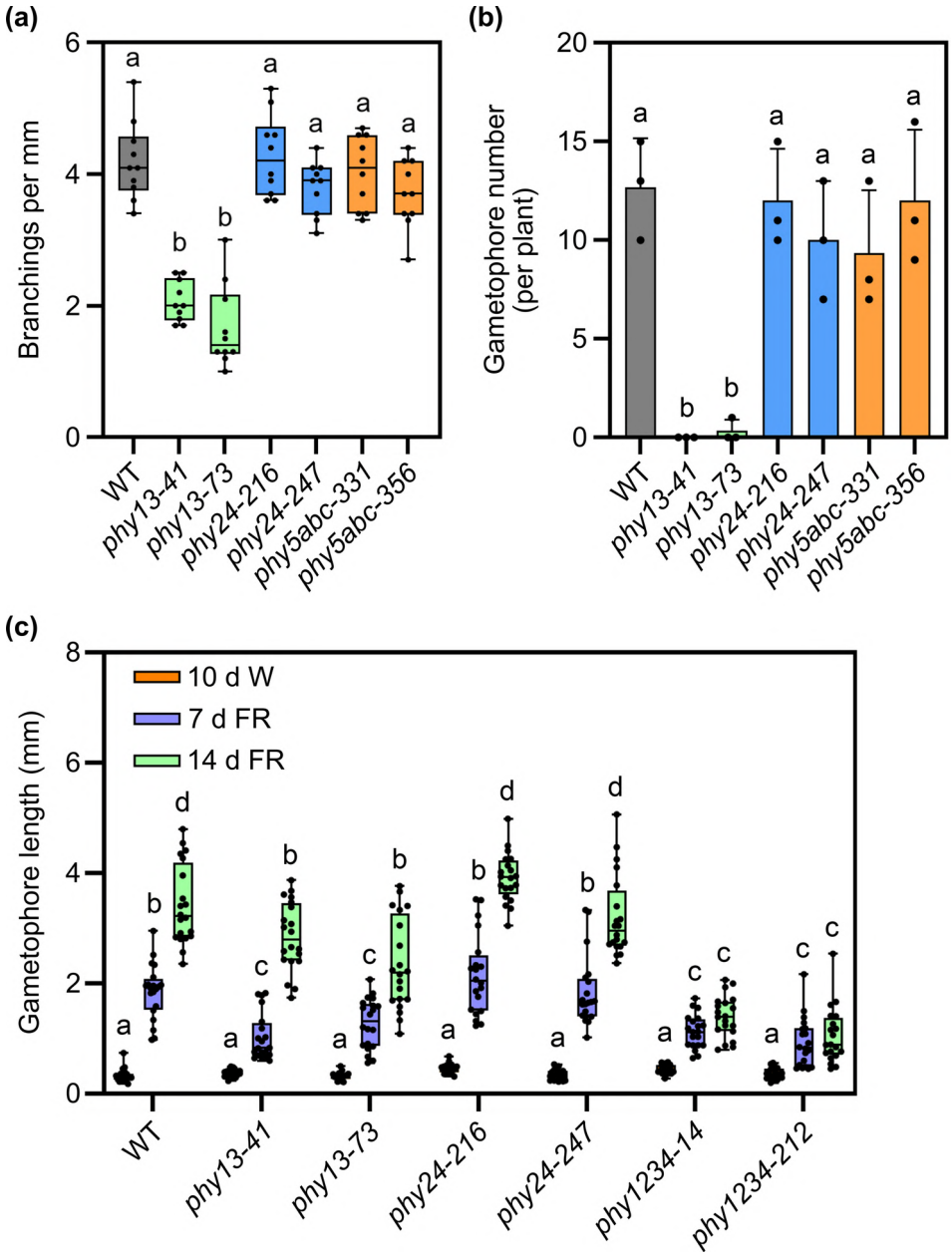

Fig. 4 Role of PHY1/3 and PHY2/4 clade phytochromes in protonema branching, gametophore induction, and gametophore growth in far-red light. (a) Protonema branching in far-red light. WT, *phy13*, *phy24*, and *phy5abc* plants (two independent lines for each mutant) were grown in far-red light (FR, 20 µmol m^{-2} s^{-1}) for 3 weeks. Branchings of protonema filaments were then counted (number of protonema filaments = 10) and length of filaments was measured. Data are shown as box plot with data points representing mean number of branchings per mm filament length; different letters indicate significant differences as determined by one-way ANOVA followed by post-hoc Tukey's HSD test; $p < 0.05$. Representative pictures of WT and mutant plants are shown in Supporting Information Fig. **S14**. (b) Gametophores were counted for WT and mutant plants grown in FR (20 µmol m^{-2} s^{-1}) for 3 weeks. Data show average number of gametophores per plant ± SD

614 (number of plants = 3); different letters indicate significant differences as determined by one-way
615 ANOVA followed by post-hoc Tukey's HSD test; $p < 0.05$. (c) Gametophore length of plants grown
616 in far-red light. Protonema of the WT and mutant lines was grown in standard growth conditions
617 (white light, W, 50 µmol m^{-2} s^{-1}) on medium supplemented with 0.5 % sucrose for 10 days to induce
618 gametophores and then transferred to FR (20 µmol m^{-2} s^{-1}) for 7 or 14 days to test for gametophore
619 growth in far-red light. Plates were incubated vertically in W and FR. The length of 20
620 gametophores was measured; data are shown as box plot; different letters indicate significant
621 differences as determined by one-way ANOVA followed by post-hoc Tukey's HSD test; $p < 0.05$.
622 Representative pictures of WT and mutant plants are shown in Supporting Information Fig. **S16**.

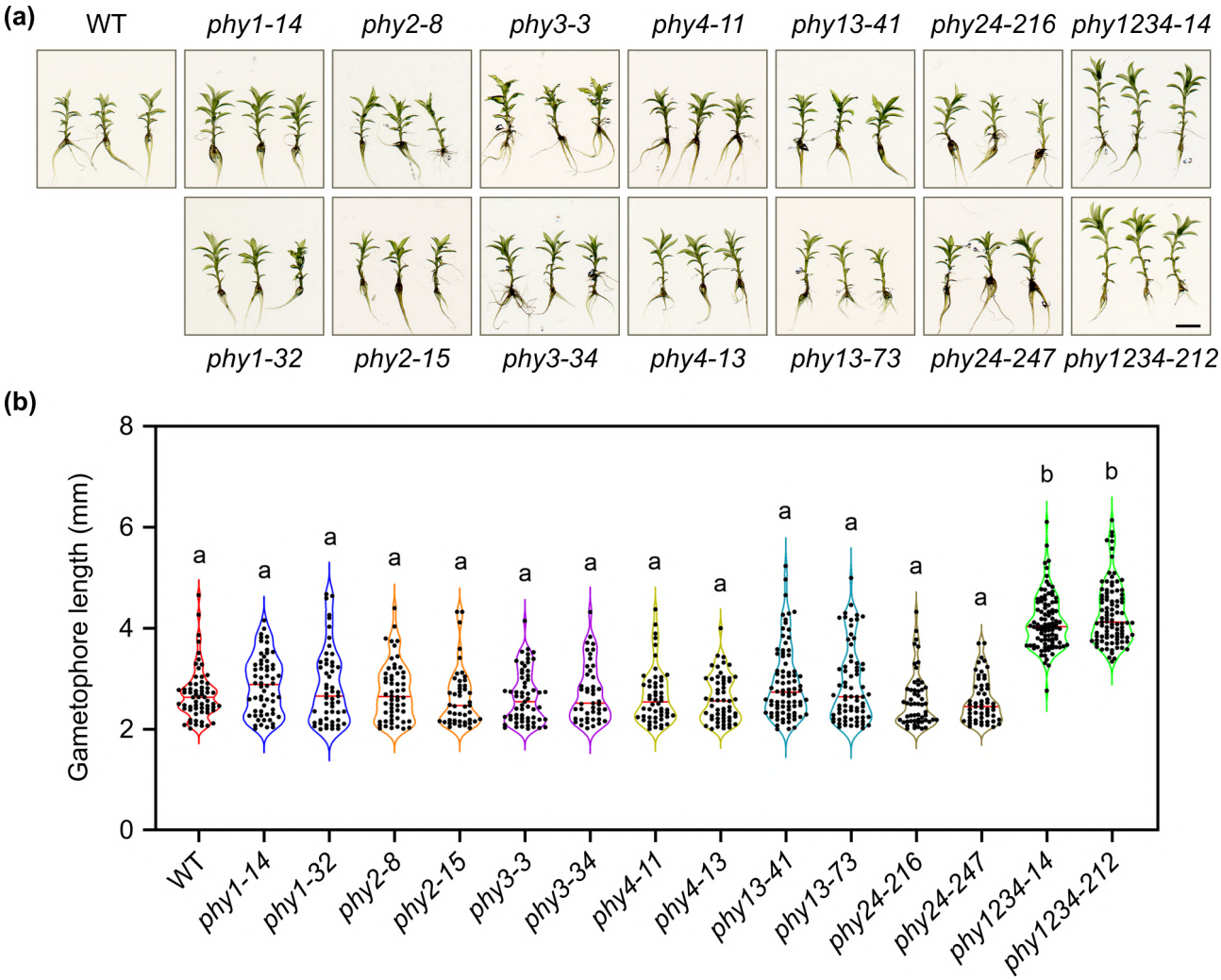

Fig. 5 The *phy1234* quadruple mutant has long gametophores in blue light. (a) Representative pictures of gametophores of WT, *phy1*, *phy2*, *phy3*, *phy4*, *phy13*, *phy24*, and *phy1234* plants (two independent lines for each mutant) grown in blue light (B, 12 µmol m^{-2} s^{-1}) for 45 days. Scale bar = 2 mm. (b) Length of gametophores was measured for WT and mutant plants grown in B (12 µmol m^{-2} s^{-1}) for 45 days. The length of ≥ 45 gametophores was measured; data are shown as violin plot; different letters indicate significant differences as determined by one-way ANOVA followed by post-hoc Tukey's HSD test; $p < 0.05$.

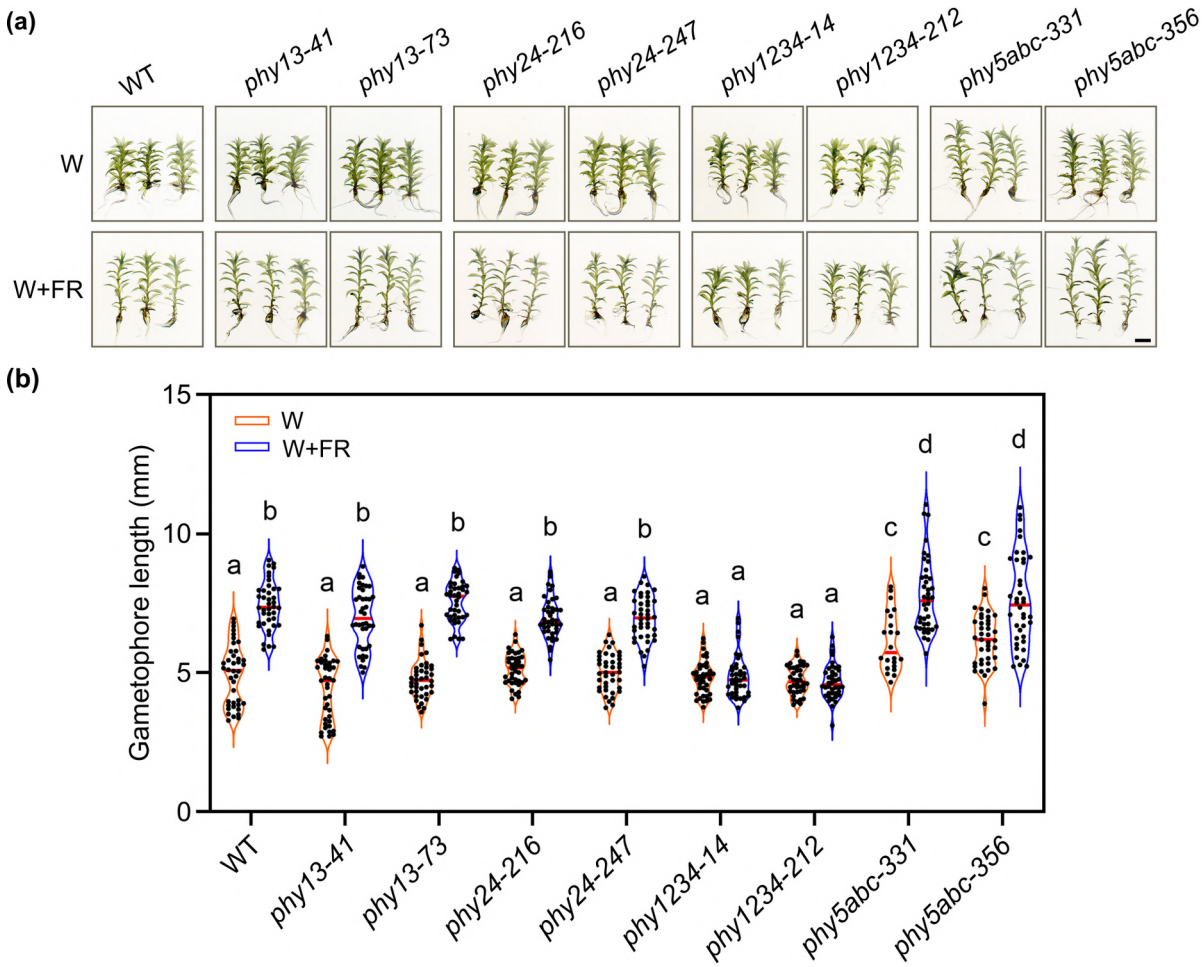

Fig. 6 Low R:FR response is impaired in the *phy1234* mutant. (a) Representative pictures of gametophores of WT, *phy13*, *phy24*, *phy1234*, and *phy5abc* plants (two independent lines for each mutant) grown in high R:FR conditions (white light without supplemental far-red light, W, 25 µmol m^{-2} s^{-1}) or low R:FR conditions (white light supplemented with far-red light, W + FR; both 25 µmol m^{-2} s^{-1}) for 45 days. Scale bar = 2 mm. (b) Length of gametophores of WT and mutant plants grown for 45 days in high (W) or low R:FR conditions (W+FR) was measured. The length of ≥ 22 gametophores was measured; data are shown as violin plot; different letters indicate significant differences as determined by two-way ANOVA followed by post-hoc Tukey's HSD test; $p < 0.05$.

Supporting Information

Article title: Phytochrome higher order mutants reveal a complex set of light responses in the moss *Physcomitrium patens*

Authors: Jinhong Yuan, Tengfei Xu, and Andreas Hiltbrunner

Article acceptance date: n/a

The following Supporting Information is available for this article:

Fig. S1 Maximum Likelihood was used to infer the phylogenetic tree of moss phytochromes.

Fig. S2 PHY1/3, PHY2/4, and PHY5 clade phytochromes in mosses.

Fig. S3 Spectra for light sources used in this study.

Fig. S4 CRISPR/Cas9-generated mutations in phytochrome genes.

Fig. S5 Magnifications of pictures shown in Fig. 1a.

Fig. S6 Protonema growth and branching of the *phy5abc* triple mutant in red light.

Fig. S7 Quantification of gametophore number and length of WT and mutant plants grown in white or red light.

Fig. S8 Induction and growth of gametophores of *phy1234* in white and red light.

Fig. S9 Phytochrome higher order mutants grown in red or white light.

Fig. S10 Induction and growth of gametophores in mutants deficient in PHY5 clade phytochromes exposed to white light.

Fig. S11 PHY5a and PHY1 are sufficient for gametophore induction in red and far-red light, respectively.

Fig. S12 Gametophore number and length of *phy2* and *phy4* single mutants grown in white light.

Fig. S13 Phytochrome protein levels in *Physcomitrium* exposed to red or far-red light.

Fig. S14 The *phy13* mutant is affected in protonema branching and gametophore induction in far-red light.

Fig. S15 PHY1/3 clade phytochromes are required for induction of gametophores in far-red light.

Fig. S16 The *phy1234* mutant is impaired in gametophore growth in far-red light.

Fig. S17 Gametophore growth of WT and *phy1234* mutant plants in far-red light.

Fig. S18 PHY1 and PHY3 induce gametophores in far-red light.

Fig. S19 *phy1234* and *phy5abc* grown in blue light.

Fig. S20 Enhanced gametophore growth in low R:FR light is impaired in *phy1234*.

Fig. S21 *Physcomitrium* phytochromes respond to diverse light conditions and play specific and overlapping roles in sensing different light qualities.

Fig. S22 Tissue-specificity and light-regulation of expression of *Physcomitrium* phytochromes.

Table S1 gBlock fragments containing the U6 promoter and coding for the respective sgRNAs used in this study.

Table S2 Cloning of plasmid constructs and references to plasmids used in this study.

Table S3 Primers used for characterisation of *phy* mutant lines by PCR and sequencing.

Table S4 Accession numbers of genes/proteins used in this study.

Data S1 Phytochrome sequences, aligned sequences, curated sequences, and tree file for Supporting Information Fig. S1 and S2.

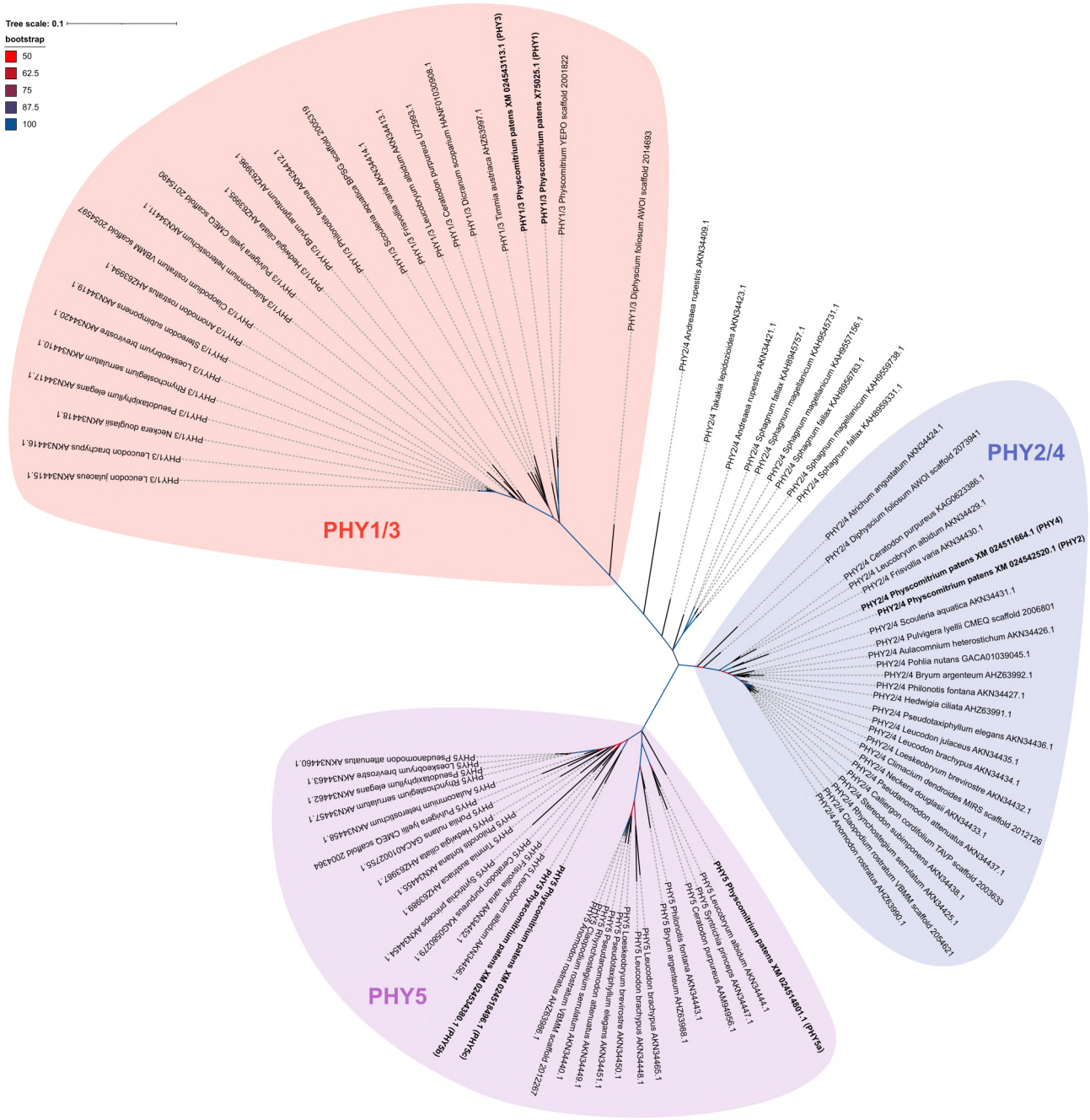

Fig. S1 Maximum Likelihood was used to infer the phylogenetic tree of moss phytochromes. Only nodes with bootstrap support ≥ 50/100 are shown. All sequences were tested in pairwise-alignments for their similarity to *Physcomitrium patens* PHY1/3, PHY2/4, and PHY5a/b/c. Sequence identifiers and *Physcomitrium patens* phytochromes to which the sequences show highest similarity are included in the leaf labels. Phytochromes belonging to Bryopsida (excludes Sphagnum, Andreaea, and Takakia) (Supporting Information Fig. **S2**), are shown on red, blue, or violet background according to their similarity to *Physcomitrium patens* phytochromes.

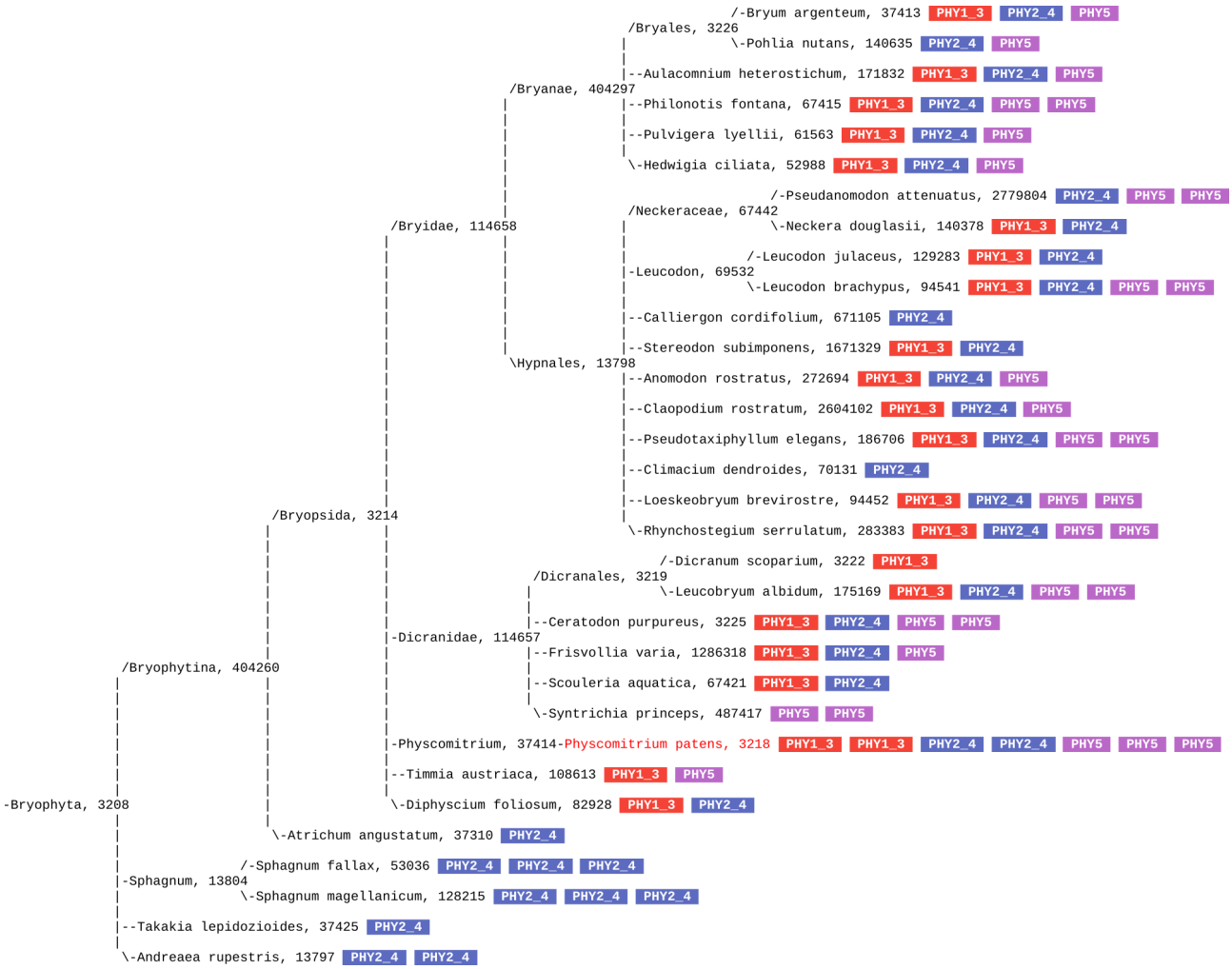

Fig. S2 PHY1/3, PHY2/4, and PHY5 clade phytochromes in mosses. Species tree for species for which at least one phytochrome sequence was found in the NCBI databases or the 1kP database (NCBI Resource Coordinators, 2013; Carpenter *et al.*, 2019). All phytochrome sequences were tested in pairwise-alignments for their similarity to *Physcomitrium patens* PHY1/3, PHY2/4, and PHY5a/b/c. Red, blue, and violet indicate highest similarity to PHY1/3, PHY2/4, and PHY5a/b/c, respectively. Each phytochrome is represented by either a red, blue, or violet box, depending on its similarity to *Physcomitrium patens* phytochromes and also included in the phylogenetic tree in Supporting Information Fig. **S1**. Numbers show NCBI taxids.

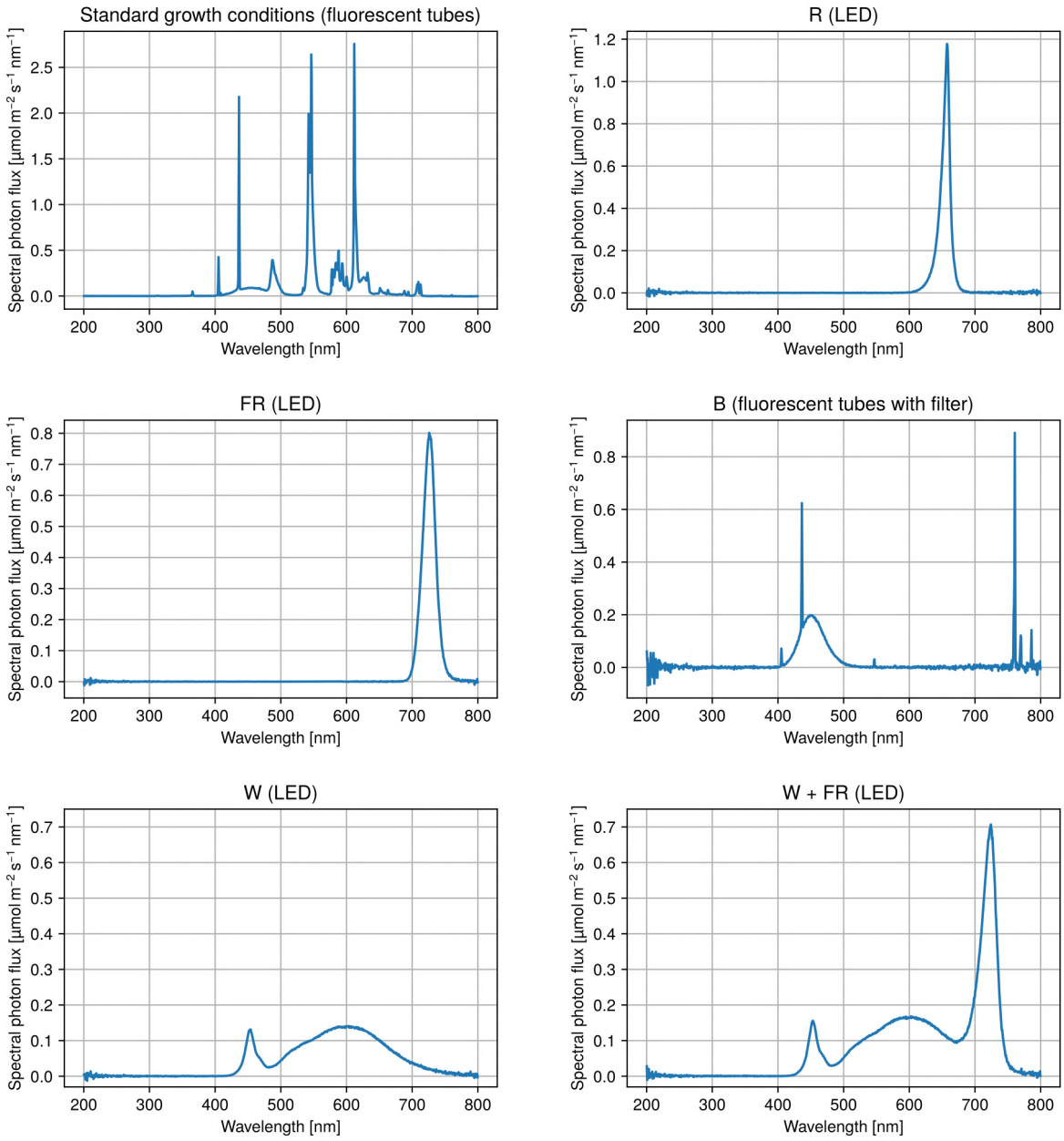

Fig. S3 Spectra for light sources used in this study. White light LEDs served as light source for the controls in the experiments involving white light supplemented with far red light (W + FR). For all other white light treatments, standard growth conditions were used.

(a)

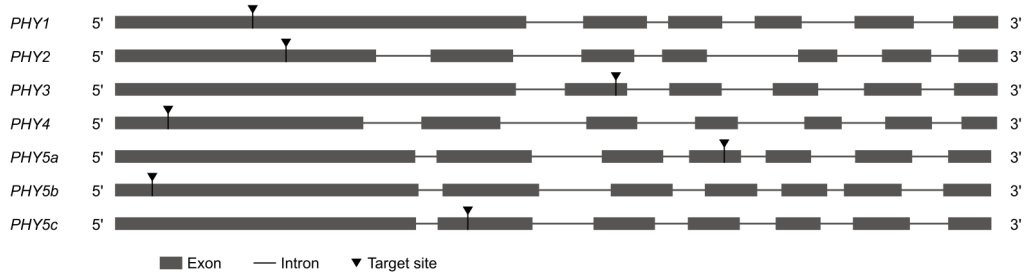

(b)

	Background	Target site and flanking region	Mutation type
PHY1			
WT		742 GGAGAGGTTGTGGCTGAGATACGT--C-----GC----------GCG-GATCTTGAGCCTTACTTAGG 791	
phy1-5	WT	GGAGAGGTTGTGGCTGAGATACGTATCTTAAGGC----------TCAAGATCTTGAGCCTTACTTAGG	-2 bp, +10 bp
phy1-14	WT	GGAGAGGTTGTGGCTGAGAT----------CTTGAGCCTTACTTAGG	-13 bp
phy1-32	WT	GGAGAGGTTGTGGCTGAGATACGT----------ATCTTGAGCCTTACTTAGG	-7 bp
phy13-41	WT	GGAGAGGTTGTGGCTGAGATAC----------GCG-GATCTTGAGCCTTACTTAGG	-5 bp
phy13-73	WT	GGAGAGGTTGTGGCTGAGATACGT----------ATCTTGAGCCTTACTTAGG	-7 bp
phy124-215	*phy24-247*	GGAGAGGTTGTGGCTGAGATACGT--C-----GCGCGGATCCGCGCG-GATCTTGAGCCTTACTTAGG	+10 bp
phy124-230	*phy24-247*	GGAGAGGTTGTGGCTGAGATA----------TCTTGGGCCTTACTTAGG	-12 bp, +1 bp
phy1234-14	WT	GGAGAGGTTGTGGCTGAGATACGT----------ATCTTGAGCCTTACTTAGG	-7 bp
phy1234-212	WT	GGAGAGGTTGTGGC----------GCG-GATCTTGAGCCTTACTTAGG	-13 bp
phy135abc-7	*phy5abc-356*	GGAGAGGTTGTGGCTGAGATAC----------GCG-GATCTTGAGCCTTACTTAGG	-5 bp
phy135abc-14	*phy5abc-356*	GGAGAGGTTGTGGCTGAGATACGT----------ATCTTGAGCCTTACTTAGG	-7 bp
PHY2			
WT		927 CAGTCTTGCGGGATCTACATTACGCGCTCCTCACGGTTGCCATGCGCAGT 976	
phy2-8	WT	CAGTCTTGCGGGATCTAC----------GTTGCCATGCGCAGT	-17 bp
phy2-15	WT	CAGTCTTGCGGGATCTACATTACGCG----------TTGCCATGCGCAGT	-10 bp
phy24-216	WT	CAGTCTTGCGGGATCTACA----------TCACGGTTGCCATGCGCAGT	-11 bp
phy24-247	WT	CAGTCTTGCGGGATCTACA----------TCACGGTTGCCATGCGCAGT	-11 bp
phy1234-14	WT	CAGTCTTGCGGGATCTACA----------TCACGGTTGCCATGCGCAGT	-11 bp
phy1234-212	WT	CAGTCTTGCGGGATCTACA----------TCACGGTTGCCATGCGCAGT	-11 bp
phy245abc-3	*phy5abc-356*	CAGTCTTGCGGGATCTACA----------TCACGGTTGCCATGCGCAGT	-11 bp
phy245abc-13	*phy5abc-356*	CAGTCTTGCGGGATCTACATTACGCG-----CACGGTTGCCATGCGCAGT	-5 bp
PHY3			
WT		2495 GCAGAATCCTCACCCTCTCATCCCTCC------T--------ATTTTTGGTGCGGACGAATTTG 2544	
phy3-3	WT	GCAGAATCCTCAGC----------GTTTGGTGCGGACGAATTTG	-18 bp, +2 bp
phy3-21	WT	GCAGAATCCTCACCCTCTCATCCCTCCAAAA--A--------ATTTTTGGTGCGGACGAATTTG	-1 bp, +5 bp
phy3-34	WT	GCAGAATCCTCACCCTCTCATCGATG----------A------GTGCGGACGAATTTG	-11 bp, +3 bp
phy13-41	WT	GCAGAATCCTCACCCTCTCA----------A--------AAATTTGGTGCGGACGAATTTG	-10 bp, +3 bp
phy13-73	WT	GCAGAATCCTCACCCTCTCATCCCACCAAAAATTAGGTATTCATTTTTGGTGCGGACGAATTTG	-1 bp, +15 bp
phy234-3	*phy24-247*	GCAGAATCCTCACCCTCTCAT----------ATTTTTGGTGCGGACGAATTTG	-7 bp
phy234-119	*phy24-216*	GCAGAATCCTCACCCTCTC----------TTTTTGGTGCGGACGAATTTG	-10 bp
phy1234-14	WT	GCAGAATCCTCACCCTCTC----------TTTTTGGTGCGGACGAATTTG	-10 bp
phy1234-212	WT	GCAGAATCCTCACCCTCTCATCCC----------ATTTTTGGTGCGGACGAATTTG	-4 bp
phy135abc-7	*phy5abc-356*	GCAGAATCCTCACCCTCTCA----------ATTTG	-25 bp
phy135abc-14	*phy5abc-356*	GCAGAATCCTCACCCTCTCA----------ATTTG	-25 bp
PHY4			
WT		304 GCGCCAGAGATGCTTGACCTGATGCCACAAGCGGTGCCCAGTGTGGGTCA 353	
phy4-11	WT	GCGCCAGAGATGCTTGACCTGATGCCA-------T---CAGTGTGGGTCA	-10 bp
phy4-13	WT	GCGCCAGAGATGCTTGACCTGATG----------TGGGTCA	-19 bp
phy24-216	WT	GCGCCAGAGATGCTTGACCTGATGCCAC------T-----GTGTGGGTCA	-11 bp
phy24-247	WT	GCGCCAGAGATGCTTGACCTGATG----------CCAGTGTGGGTCA	-13 bp
phy1234-14	WT	GCGCCAGAGATGCTTGACCTGATGCCAC------T-----GTGTGGGTCA	-11 bp
phy1234-212	WT	GCGCCAGAGATGCTTGACCTGATGCCAC------T-----GTGTGGGTCA	-11 bp
phy245abc-3	*phy5abc-356*	GCGCCAGAGATGCTTGACCTGATGCCA--AGCGGTGCCCAGTGTGGGTCA	-2 bp
phy245abc-13	*phy5abc-356*	GCGCCAGAGATGCTTGACCTGATGCCA--AGCGGTGCCCAGTGTGGGTCA	-2 bp

(Fig. S4 — continued on next page)

(Fig. S4 — continued from previous page)

PHY5a

WT		3131	GAGCTCTGCTTACGGCTAACAAG-AGAACG--GA----TGCAGATGGAT--A----CATCAC	3180
phy5a-741	WT		GAGCTCTGCTTACGGCTAACAAG-A----------TGCAGATGGAT--A----CATCAC	-7 bp
phy5a-762	WT		GAGCTCTGCTTACGGCTAACAAGGTGTTTTTTGCTTTCTGCAGATGTATCCATCTGCATCAC	-8 bp, +21 bp
phy5ab-701	WT		GAGCTCTGCTTACGGCTAACAAG-A----------TGGAT--A----CATCAC	-13 bp
phy5ab-777	WT		GAGCTCTGCTTACGGCTAACA---AGAACG--GA----TGCAGATGGAT--A----CATCAC	-2 bp
phy5ac-18	WT		GAGCTCTGCTTACGGCTAACAAG-A----------TGCAGATGGAT--A----CATCAC	-7 bp
phy5ac-32	WT		GAGCTCTGCTTACGGCTAACAAG-A----------TGCAGATGGAT--A----CATCAC	-7 bp
phy5abc-331	WT		GAGCTCTGCTTACGGCTAACAAG-A----------TGCAGATGGAT--A----CATCAC	-7 bp
phy5abc-356	WT		GAGCTCTGCTTACGG----------AT--A----CATCAC	-25 bp
phy2345abc-230	*phy234-119*		GAGCTCTGCTTACGGCTAACAAG----------CAGATGGAT--A----CATCAC	-10 bp
phy2345abc-272	*phy234-119*		GAGCTCTGCTTACGGCTAACAAG-A----------TGGAT--A----CATCAC	-13 bp
phy12345abc-5	*phy12345bc-24*		G----------T--A----CATCAC	-40 bp
phy12345abc-13	*phy12345bc-24*		GAGCTCTGCTTACGGCTAACAAG-A----------TGCAGATGGAT--A----CATCAC	-7 bp

PHY5b

WT		353	GTCTAAAGGAAGTCCTCGGAATCGGAACCGA----------T-GCGAGGTTGTTGTTCACT	402
phy5b-704	WT		GTCTAAAGGAAGTCCTCGGAATCGGAACCGA----------TTGCGAGGTTGTTGTTCACT	+1 bp
phy5b-745	WT		GTCTAAAGGAAGTCCTCGGAATCGGAACCGA----------GGTTGTTGTTCACT	-5 bp
phy5ab-701	WT		GTCTAAAGGAAGTCCTCGGAATCGGAACCGA----------T-T----GTTGTTGTTCACT	-5 bp, +1 bp
phy5ab-777	WT		GTCTAAAGGAAGTCCTCGGAATCG----------GTTGTTGTTCACT	-13 bp
phy5bc-23	WT		GTCTAAAGGAAGTCCTCGGAATCGGAACCGAGGACAGGGACGACAGTCGGAATTGCGAGGTTGTTGTTCACT	+22 bp
phy5bc-70	WT		GTCTAAAGGAAGTCCTCGGAA----------GCGAGGTTGTTGTTCACT	-11 bp
phy5abc-331	WT		GTCTAAAGGAAGTCCTCGGAATCGGAACCGA----------T----------TGTTCACT	-10 bp
phy5abc-356	WT		GTCTAAAGGAAGTCCTCGGAATCGG----------TTCACT	-19 bp
phy12345bc-11	*phy1234-212*		GTCTAAAGGAAGTCCTCGGAATCGGAACCGA----------T--------TGTTGTTCACT	-7 bp
phy12345bc-24	*phy1234-212*		GTCTAAAGGAAGTCCTCGGAATCGGAACCGA----------GGTTGTTGTTCACT	-5 bp
phy2345abc-230	*phy234-119*		GTCTAAAGGAAGTCCTCGGAA----------GCGAGGTTGTTGTTCACT	-11 bp
phy2345abc-272	*phy234-119*		GTCTAAAGGAAGTCCTCGGAATCGGAACCGA----------GGTTGTTGTTCACT	-5 bp

PHY5c

WT		1863	GACGATAGCGATGGGAAAACGATGATTCAT--------GCGCGGCTTCACGATTTGAA	1912
phy5c-3	WT		GACGATAGCGATGGGAAAACG----------TTTGAA	-23 bp
phy5c-24	WT		GACGATAGCGATGGGAAAACGAT----------TTGAA	-22 bp
phy5ac-18	WT		GACGATAGCGATGGGAAAACGATGATTCATCGTTTTCAGCGCGGCTTCACGATTTGAA	+8 bp
phy5ac-32	WT		GACGATAGCGATGGGAAACC----------GCGCGGCTTCACGATTTGAA	-11 bp, +1 bp
phy5bc-23	WT		GACGATAGCGATGGGAAAACGATGATTCAT----------CGTTTTGAA	-12 bp, +1 bp
phy5bc-70	WT		GACGATAGCGATGGGAAAACGAT----------TTGAA	-22 bp
phy5abc-331	WT		GACGATAGCGATGGGAAAACGAT----------TTGAA	-22 bp
phy5abc-356	WT		GACGATA----------GCGCGGCTTCACGATTTGAA	-23 bp
phy12345bc-11	*phy1234-212*		GACGATAGCGATGGGAAAACGATGATTCAT----------C-GCTTCACGATTTGAA	-4 bp
phy12345bc-24	*phy1234-212*		GACGATAGCGATGGGAAAACGATGATTCAT----------CGATTTGAA	-11 bp
phy2345abc-230	*phy234-119*		GACGATAGCGATGGGAAAACGAT----------TTGAA	-22 bp
phy2345abc-272	*phy234-119*		GACGATAGCGATGGGAAAACGATGATTCAAATCGTGAAGCGCGGCTTCACGATTTGAA	+8 bp

Fig. S4 CRISPR/Cas9-generated mutations in phytochrome genes. (a) Schematic representation of the *PHY1-5c* genomic loci and positions of CRISPR/Cas9 target sites (black triangles). (b) Sequence alignment for target sites and flanking regions in WT and CRISPR/Cas9-generated *phy* mutant alleles. Target sites are shown in blue, deletions are represented by orange dashes, and insertions are highlighted in purple. Part of the mutants is derived from other mutants; the background used for mutagenesis is indicated.

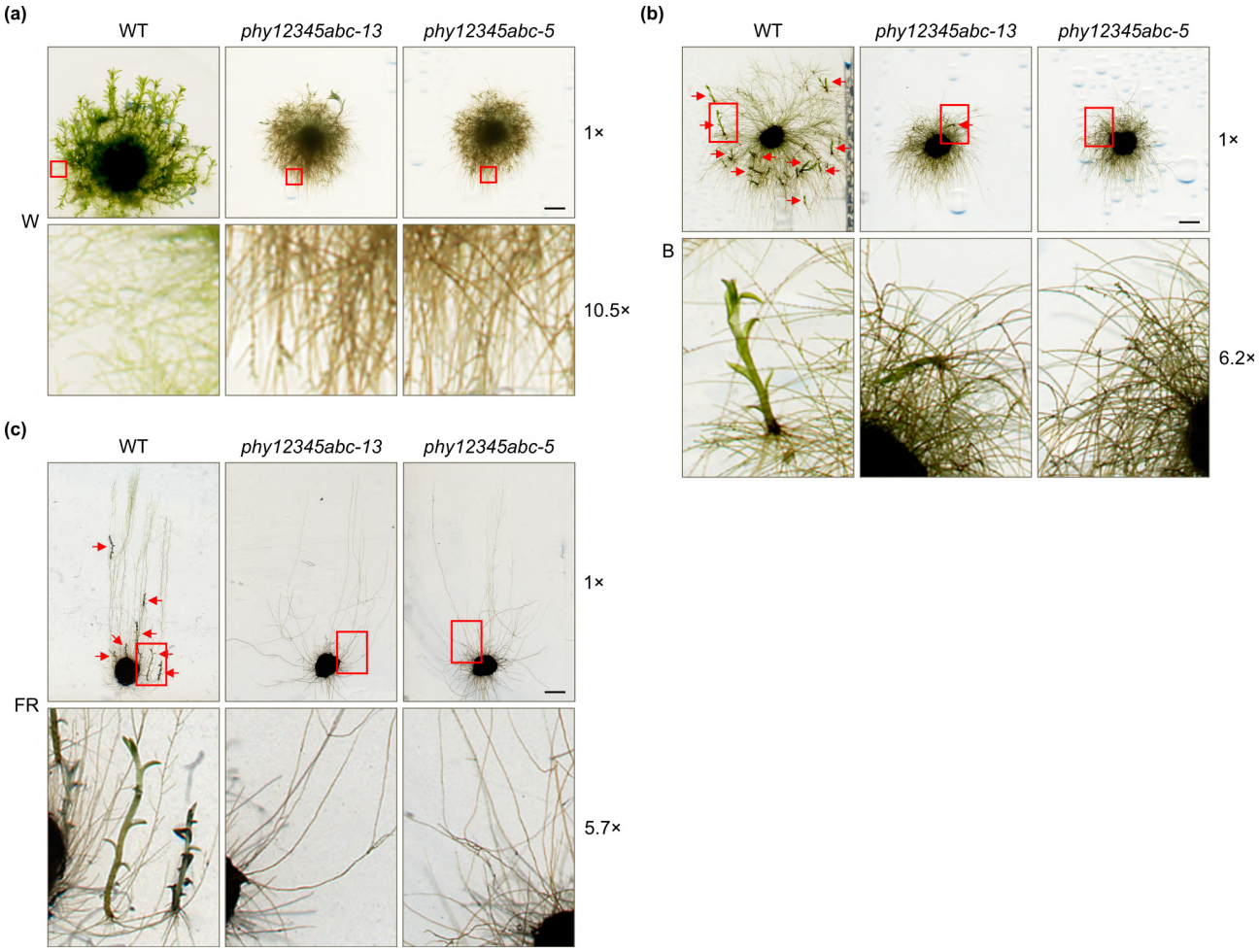

Fig. S5 Magnifications of pictures shown in Fig. **1a**. (a)-(c) WT and two independent *phy12345abc* septuple mutant lines were vertically grown in (a) standard growth conditions (white light, W, 50 µmol m^{-2} s^{-1}), (b) blue light (B, 12 µmol m^{-2} s^{-1}), or (c) far-red light (FR, 20 µmol m^{-2} s^{-1}) for 45 days. Scale bar = 2 mm. Red squares indicate magnified areas; magnification is shown on the right of the respective pictures. Red arrows point to gametophores of plants grown in B or FR.

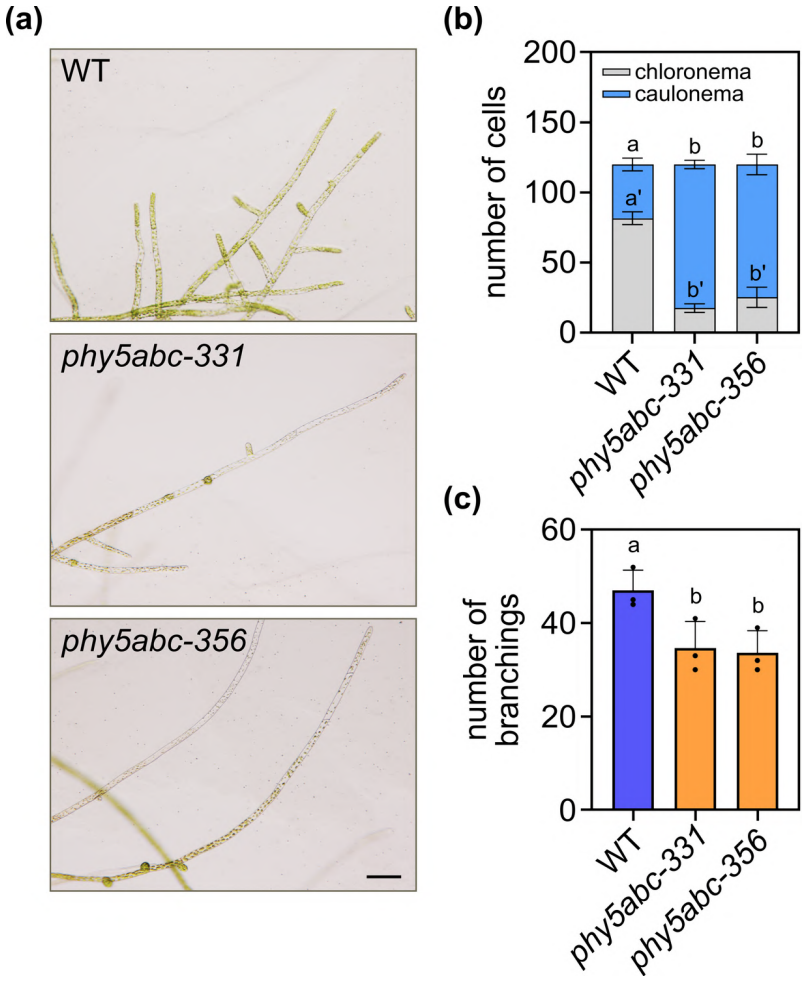

Fig. S6 Protonema growth and branching of the *phy5abc* triple mutant in red light. (a) Freshly fragmented protonema tissue of the WT and two independent *phy5abc* triple mutant lines was spotted onto solid Knop's medium supplemented with 0.5 % sucrose and cultivated in red light (R, 20 µmol m^{-2} s^{-1}) for 14 days. Pictures were taken by stereo microscopy. Scale bar = 100 µm. (b) Caulonemal and chloronemal cells were counted within the six cells from the tip of twenty protonema filaments. Different letters indicate significant differences as determined by one-way ANOVA followed by post-hoc Tukey's HSD test; $p < 0.05$. Error bars show ± SD. (c) Protonema branching. Branchings within the six cells from the tip of twenty protonema filaments were counted. Data points show mean number of branchings of three replicates ± SD. Different letters indicate significant differences as determined by one-way ANOVA followed by post-hoc Tukey's HSD test; $p < 0.05$. Error bars show ± SD.

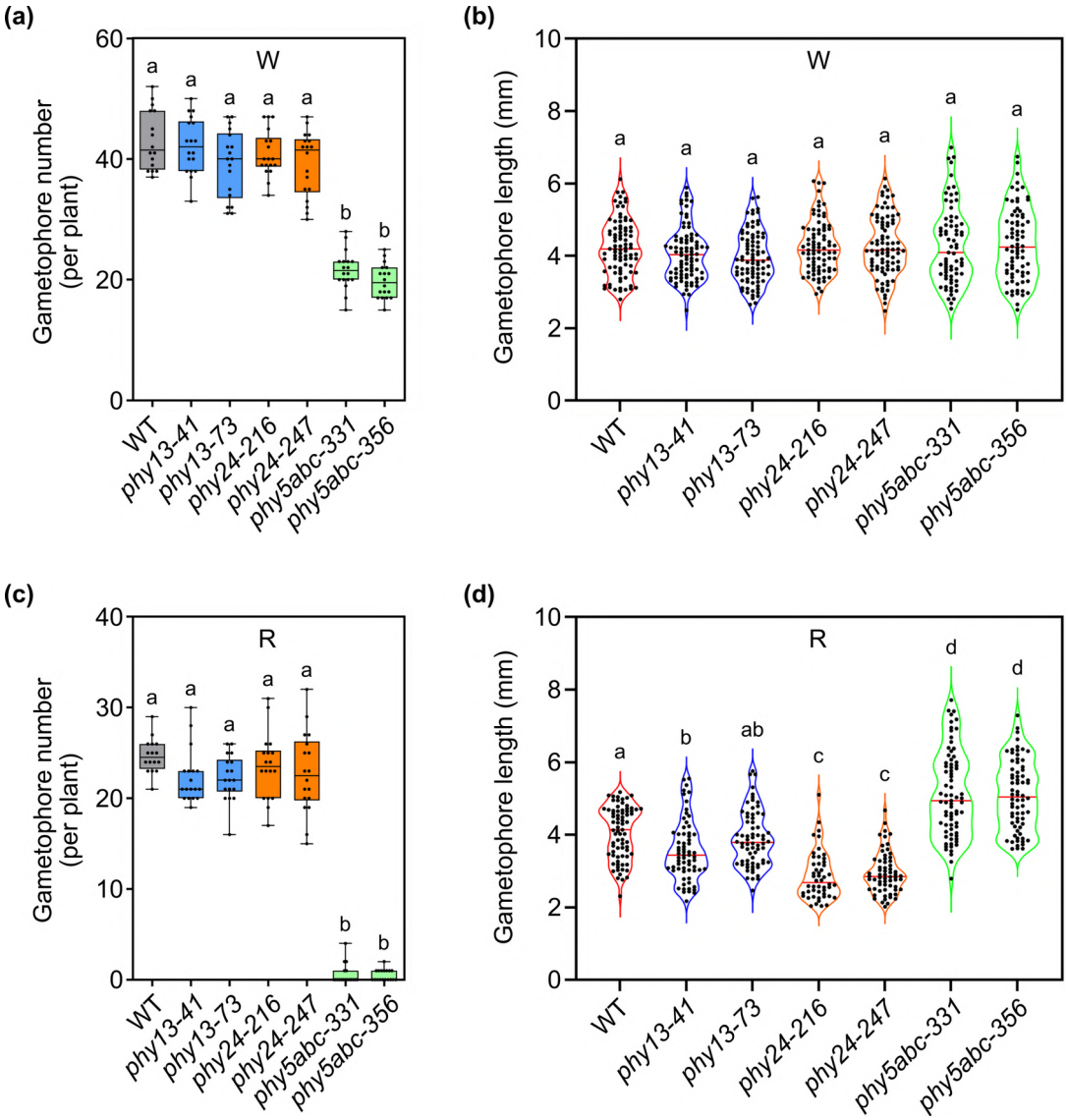

Fig. S7 Quantification of gametophore number and length of WT and mutant plants grown in white or red light. (a), (c) Gametophores were counted for WT, *phy13*, *phy24*, and *phy5abc* plants (two independent lines for each mutant) grown in (a) standard growth conditions (white light, W, 50 μmol m^{-2} s^{-1}) or (c) red light (R, 20 μmol m^{-2} s^{-1}) for 14 days. Data are shown as box plot (number of plants ≥ 16); different letters indicate significant differences as determined by one-way ANOVA followed by post-hoc Tukey's HSD test; $p < 0.05$. Representative pictures of plants are shown in Fig. **1b**. (b), (d) Length of gametophores was measured for WT and mutant plants grown in (b) standard growth conditions (W, 50 μmol m^{-2} s^{-1}) or (d) R (20 μmol m^{-2} s^{-1}) for 45 days. The length of > 50 gametophores was measured. Data are shown as violin plot; different letters indicate significant differences as determined by one-way ANOVA followed by post-hoc Tukey's HSD test; $p < 0.05$.

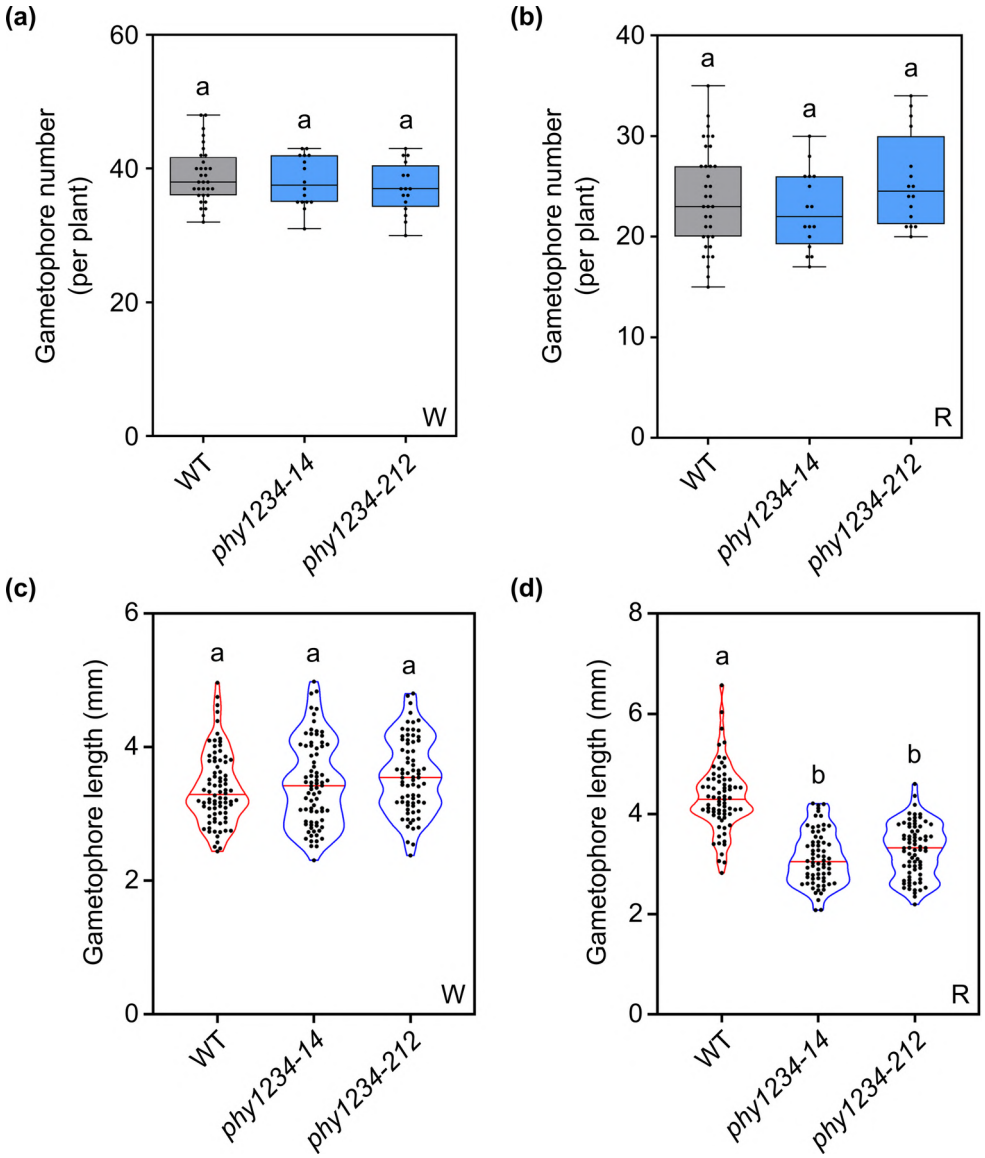

Fig. S8 Induction and growth of gametophores of *phy1234* in white and red light. (a), (b) Quantification of gametophore number for WT and two independent *phy1234* mutant lines grown in (a) standard growth conditions (white light, W, 50 µmol m^{-2} s^{-1}) or (b) red light (R, 20 µmol m^{-2} s^{-1}) for 14 days. Data are shown as box plot (number of plants ≥ 16); different letters indicate significant differences as determined by one-way ANOVA followed by post-hoc Tukey's HSD test; $p < 0.05$. (c), (d) Length of gametophores of WT and two independent *phy1234* mutant lines grown for 45 days in (c) standard growth conditions (W, 50 µmol m^{-2} s^{-1}) or (d) R (20 µmol m^{-2} s^{-1}). The length of > 60 gametophores was measured. Data are shown as violin plot; different letters indicate significant differences as determined by one-way ANOVA followed by post-hoc Tukey's HSD test; $p < 0.05$.

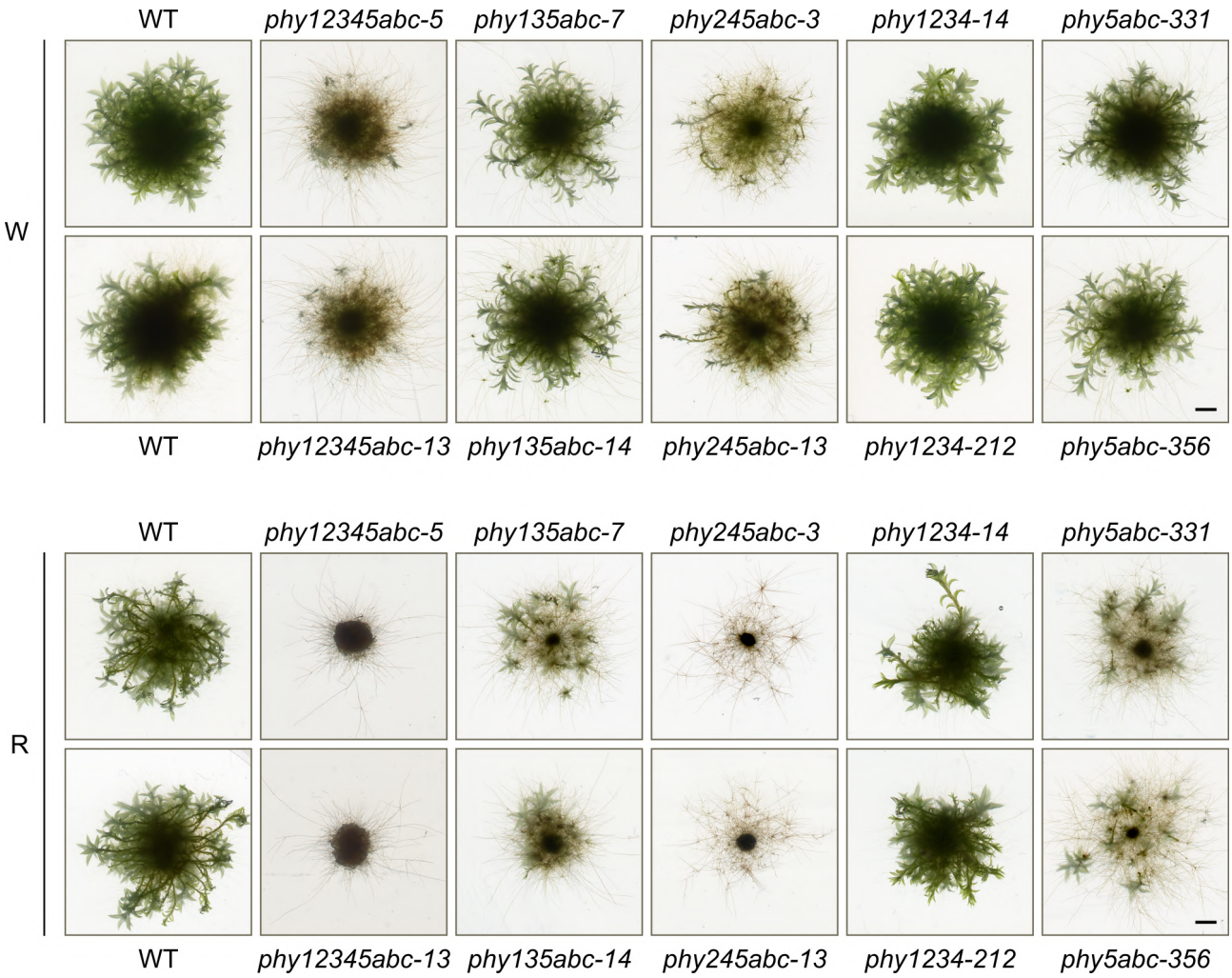

Fig. S9 Phytochrome higher order mutants grown in red or white light. Freshly fragmented protonema cultures of WT, *phy12345abc*, *phy135abc*, *phy245abc*, *phy1234*, and *phy5abc* plants (two independent lines for each mutant) were spotted onto solid Knop's medium supplemented with 0.5 % sucrose and incubated in standard growth conditions (white light, W, 50 µmol m^{-2} s^{-1}) or red light (R, 20 µmol m^{-2} s^{-1}) for 45 days. Scale bar = 2 mm.

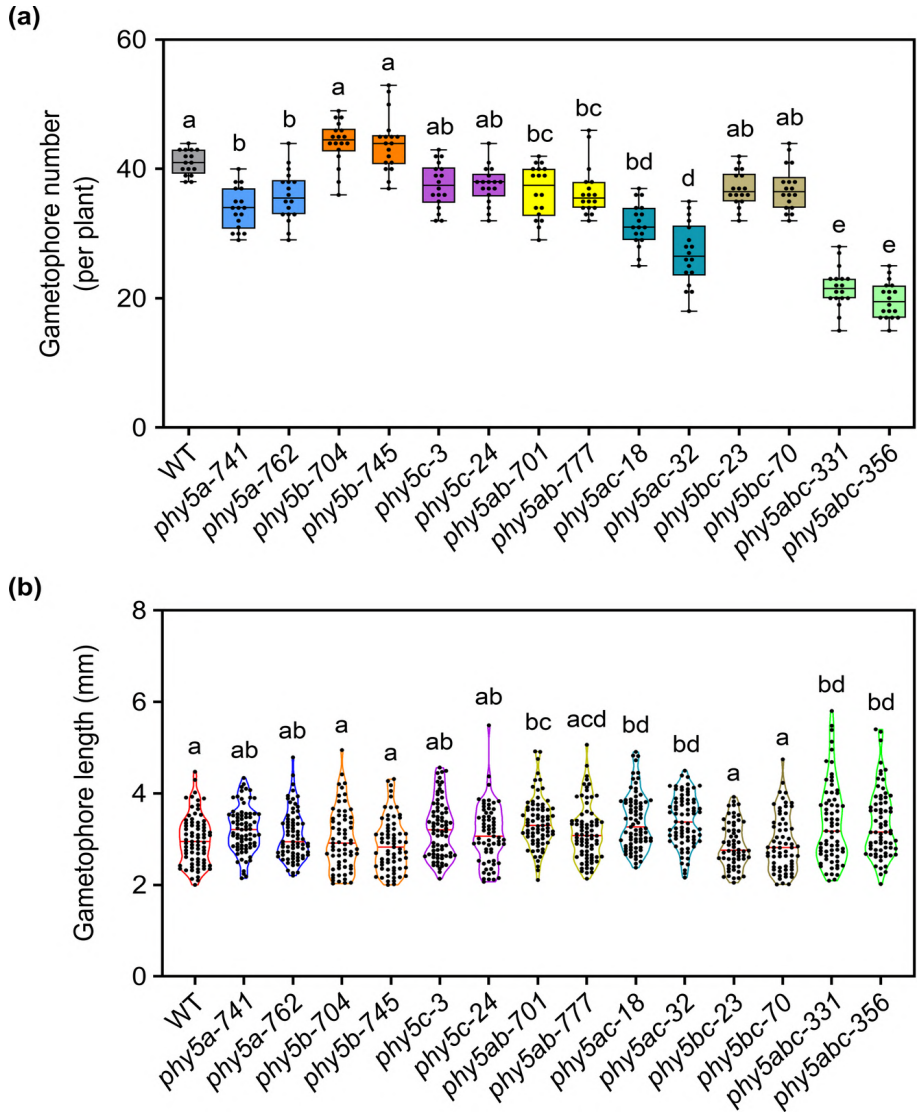

Fig. S10 Induction and growth of gametophores in mutants deficient in PHY5 clade phytochromes exposed to white light. (a) Quantification of gametophore number for WT, *phy5a, phy5b, phy5c, phy5ab, phy5ac, phy5bc,* and *phy5abc* plants grown in standard growth conditions (white light, W, 50 µmol m^{-2} s^{-1}) for 14 days. Data are shown as box plot (number of plants ≥ 16); different letters indicate significant differences as determined by one-way ANOVA followed by post-hoc Tukey's HSD test; $p < 0.05$. (b) Length of gametophores was measured for WT and mutant plants grown in standard growth conditions (white light, W, 50 µmol m^{-2} s^{-1}) for 45 days. The length of ≥ 60 gametophores was measured; data are shown as violin plot; different letters indicate significant differences as determined by one-way ANOVA followed by post-hoc Tukey's HSD test; $p < 0.05$.

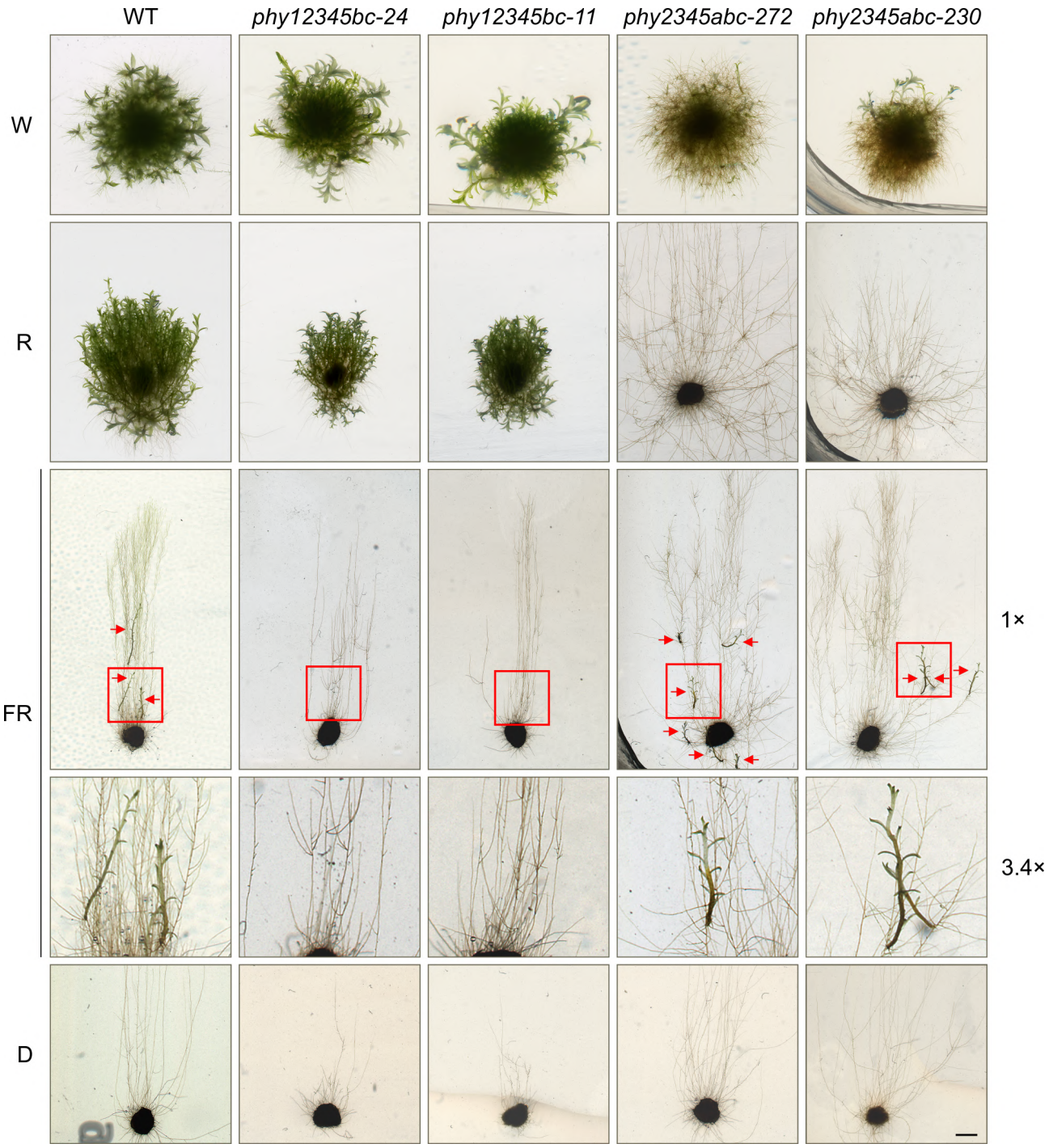

Fig. S11 PHY5a and PHY1 are sufficient for gametophore induction in red and far-red light, respectively. Freshly fragmented protonema cultures of WT, *phy12345bc*, and *phy2345abc* (two independent lines for each mutant) were spotted onto solid Knop's medium supplemented with 0.5 % sucrose. Plates were incubated vertically for 45 days in standard growth conditions (white light, W, 50 µmol m^{-2} s^{-1}), red light (R, 20 µmol m^{-2} s^{-1}), far-red light (FR, 20 µmol m^{-2} s^{-1}), or dark conditions (D). Scale bar = 2 mm. Red arrows point to gametophores of plants grown in far-red

light. Red squares indicate magnified areas; magnification is shown on the right of the respective pictures.

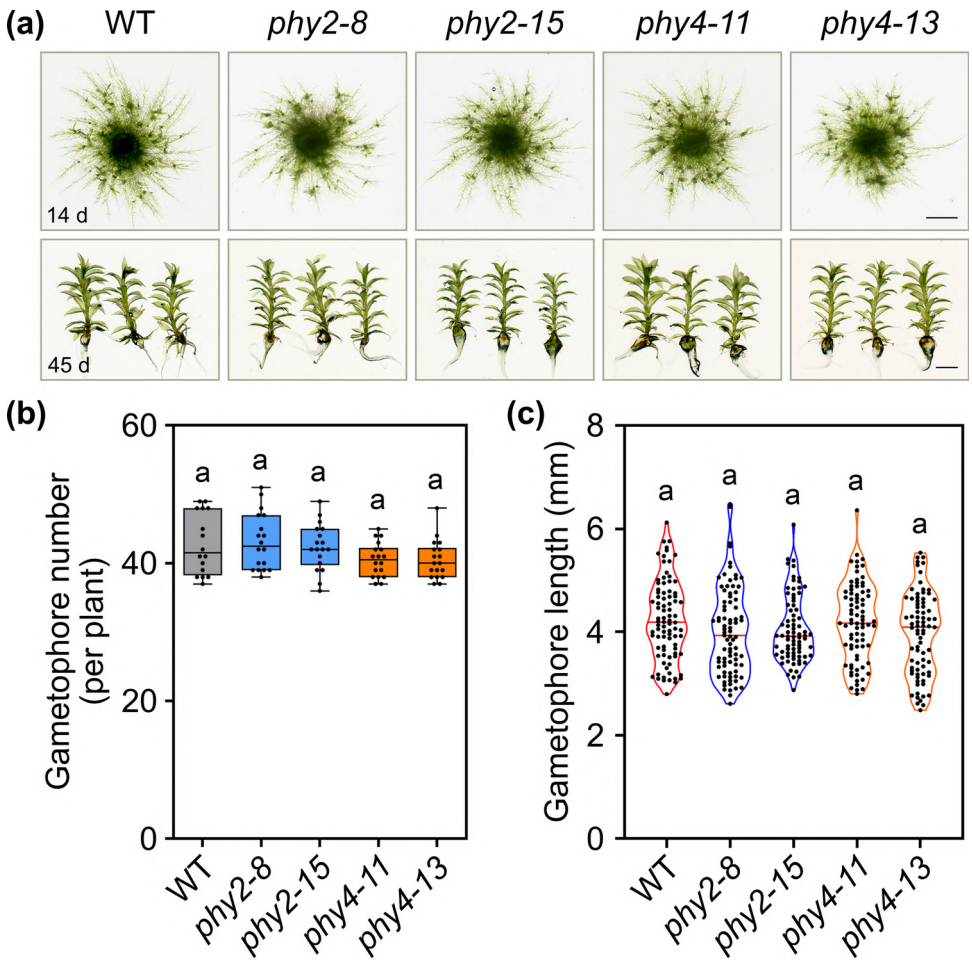

Fig. S12 Gametophore number and length of *phy2* and *phy4* single mutants grown in white light. (a) Representative pictures of WT, *phy2*, and *phy4* plants (two independent lines for each mutant) grown in standard growth conditions (white light, W, 50 µmol m^{-2} s^{-1}) for 14 days (upper row). Representative gametophores picked from plants grown for 45 days in standard growth conditions (W, 50 µmol m^{-2} s^{-1}) are shown in the lower row. Scale bar = 2 mm. (b) Quantification of gametophore number for WT, *phy2*, and *phy4* plants (two independent lines for each mutant) grown in standard growth conditions (W, 50 µmol m^{-2} s^{-1}) for 14 days. Data are shown as box plot (number of plants ≥ 16); different letters indicate significant differences as determined by one-way ANOVA followed by post-hoc Tukey's HSD test; $p < 0.05$. (c) Length of gametophores of WT and mutant plants grown for 45 days in standard growth conditions (W, 50 µmol m^{-2} s^{-1}). The length of > 60 gametophores was measured; data are shown as violin plot; different letters indicate significant differences as determined by one-way ANOVA followed by post-hoc Tukey's HSD test; $p < 0.05$.

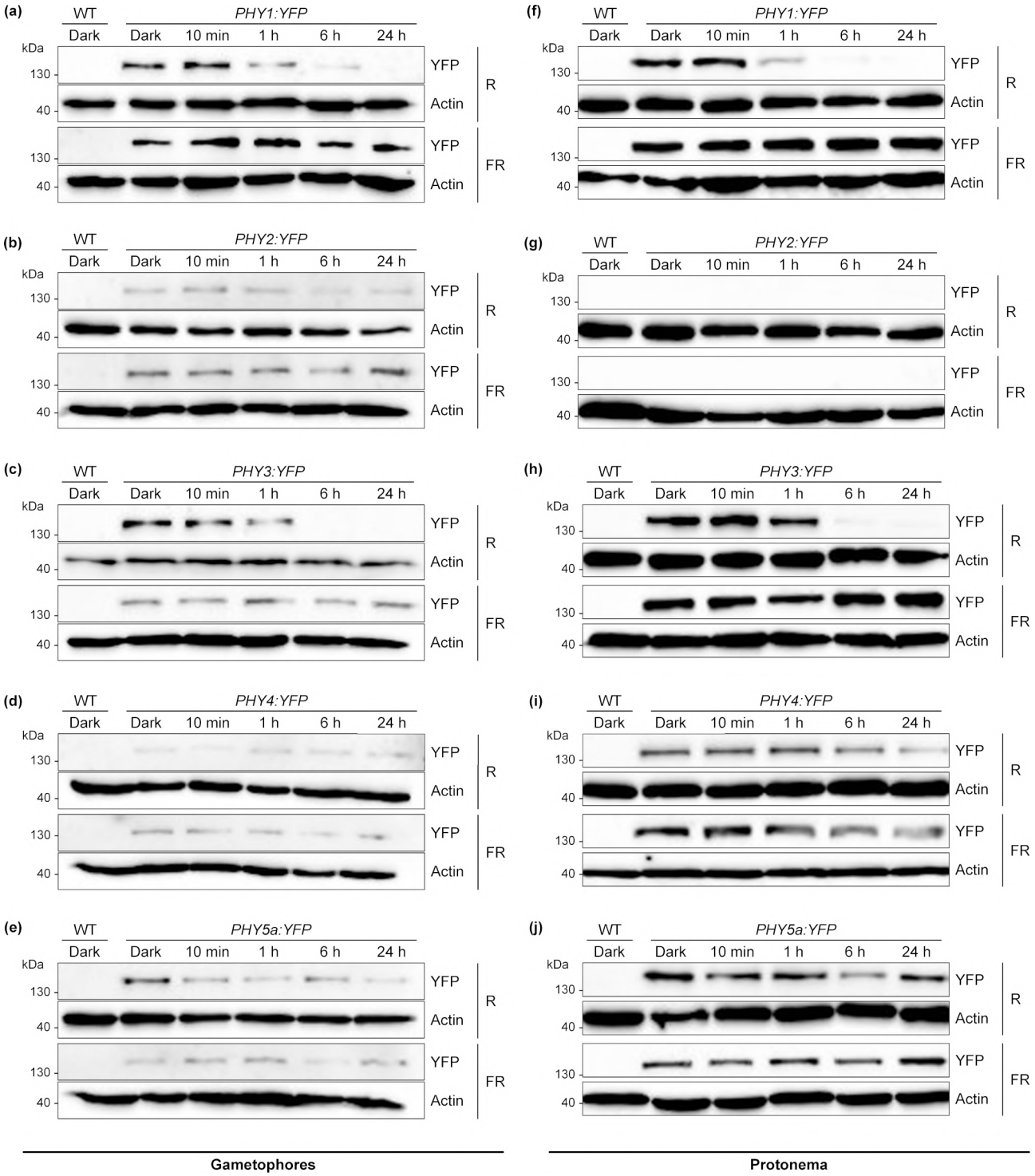

Fig. S13 Phytochrome protein levels in *Physcomitrium* exposed to red or far-red light. (a)-(e) Gametophore cultures of lines expressing endogenous *PHY1*, *PHY2*, *PHY3*, *PHY4*, or *PHY5a* fused to the coding sequence of YFP (i.e. the coding sequence of YFP has been inserted into the genome downstream of the last codon of the respective endogenous phytochrome; Possart & Hiltbrunner, 2013) were grown in standard growth conditions (white light, W, 50 µmol m^{-2} s^{-1}) and

subsequently transferred to dark for 4 days for dark adaptation. Then plants were exposed to red light (R, 20 µmol m^{-2} s^{-1}) or far-red light (FR, 20 µmol m^{-2} s^{-1}) for different time periods. Total protein was extracted and analysed by SDS-PAGE and immunoblotting with anti-GFP antibody. Protein extracts from dark-adapted wild type gametophore cultures were used as negative controls. Actin is shown as a loading control. (f)-(j) Protonema cultures were incubated in standard growth conditions (W, 50 µmol m^{-2} s^{-1}) for 10 days and subsequently transferred to dark conditions for 4 days for dark adaptation. Light treatment and immunoblot analysis was done as described for (a)-(e). PHY2-YFP in protonema samples was below detection limits.

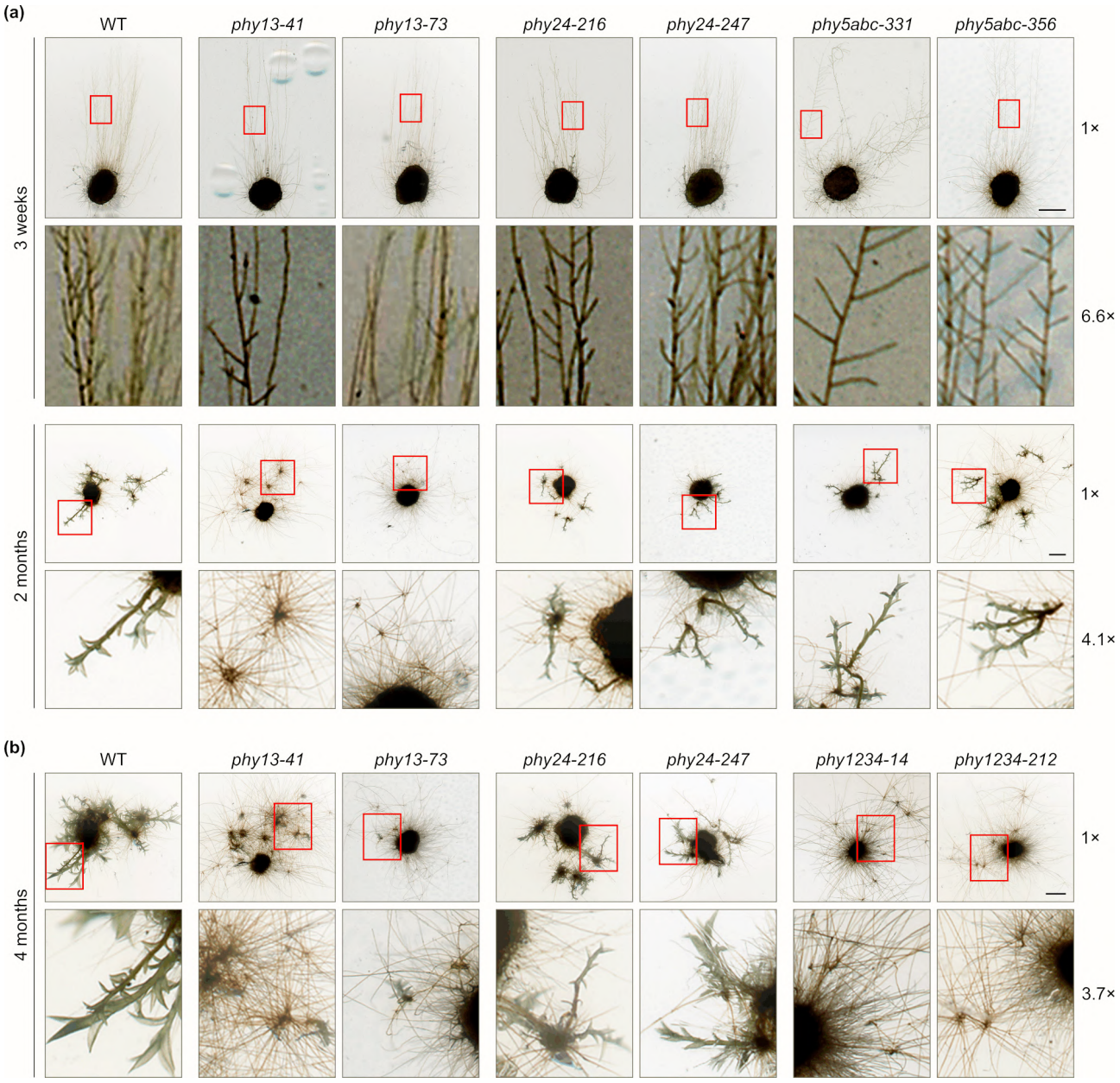

Fig. S14 The *phy13* mutant is affected in protonema branching and gametophore induction in far-red light. (a) Representative pictures of protonema cultures of WT, *phy13*, *phy24*, and *phy5abc* plants (two independent lines for each mutant) grown in far-red light (FR, 20 µmol m^{-2} s^{-1}) for 3 weeks (upper row, plates were vertically incubated) or 2 months (lower row) on medium supplemented with 0.5 % sucrose. (b) Representative pictures of WT, *phy13*, *phy24*, and *phy1234* plants (two independent lines for each mutant) grown in FR (20 µmol m^{-2} s^{-1}) for 4 months on medium supplemented with 0.5 % sucrose. (a), (b) Scale bar = 2 mm. Red squares indicate magnified areas; magnification is shown on the right of the respective pictures. Quantification of protonema branching and gametophore number is shown in Fig. **4a, b**.

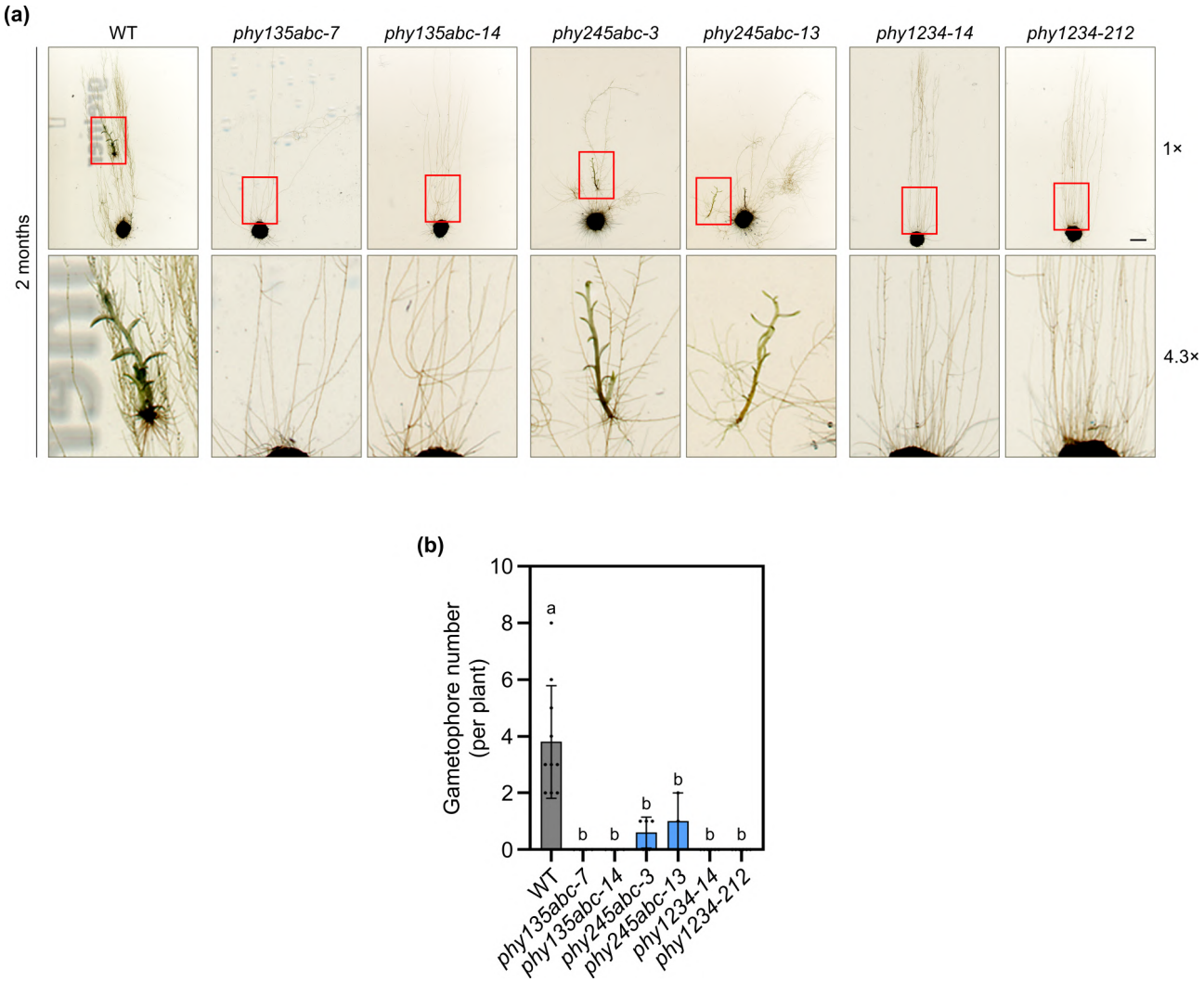

Fig. S15 PHY1/3 clade phytochromes are required for induction of gametophores in far-red light. (a) Representative pictures of protonema cultures of WT, *phy135abc*, *phy245abc*, and *phy1234* plants (two independent lines for each mutant) vertically grown in far-red light (20 µmol m^{-2} s^{-1}) for 2 months on medium supplemented with 0.5 % sucrose. Scale bar = 2 mm. Red squares indicate magnified areas; magnification is shown on the right of the respective pictures. (b) Quantification of gametophore number. Data show mean gametophore number ± SD (number of plants ≥ 3); different letters indicate significant differences as determined by one-way ANOVA followed by post-hoc Tukey's HSD test; $p < 0.05$.

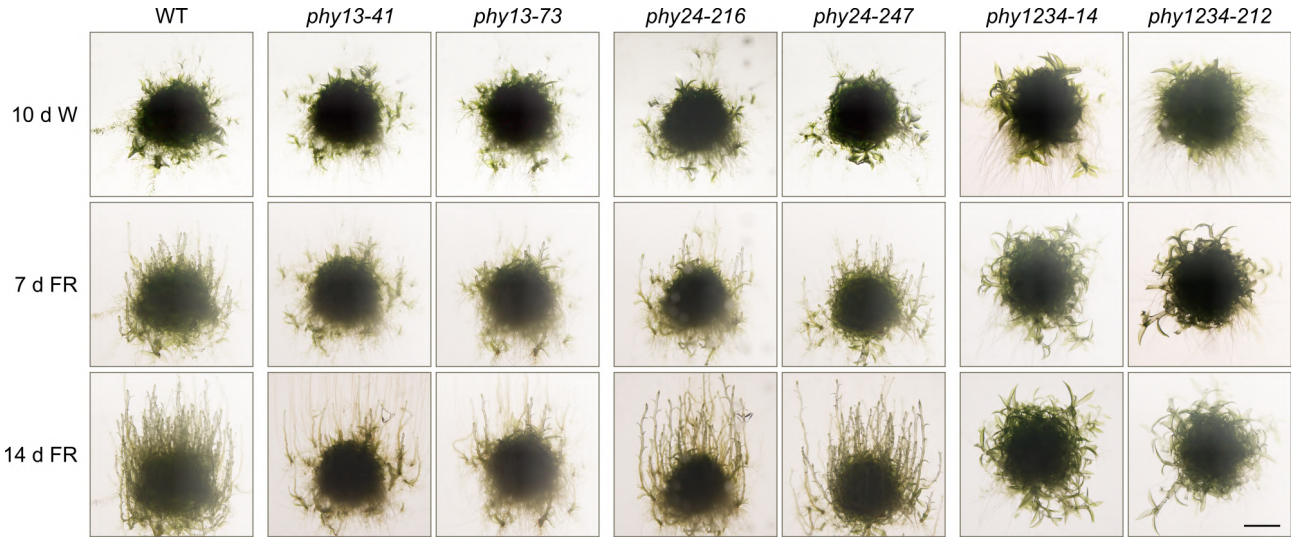

Fig. S16 The *phy1234* mutant is impaired in gametophore growth in far-red light. Protonema of WT, *phy13*, *phy24*, and *phy1234* plants (two independent lines for each mutant) was grown in standard growth conditions (white light, W, 50 µmol m^{-2} s^{-1}) on medium supplemented with 0.5 % sucrose for 10 days to induce gametophores and then transferred to far-red light (FR, 20 µmol m^{-2} s^{-1}) for 7 or 14 days to test for gametophore growth in FR. Plates were incubated vertically in W or FR. Representative pictures of plants are shown. Scale bar = 2 mm. Quantification of gametophore length is shown in Fig. **4c**.

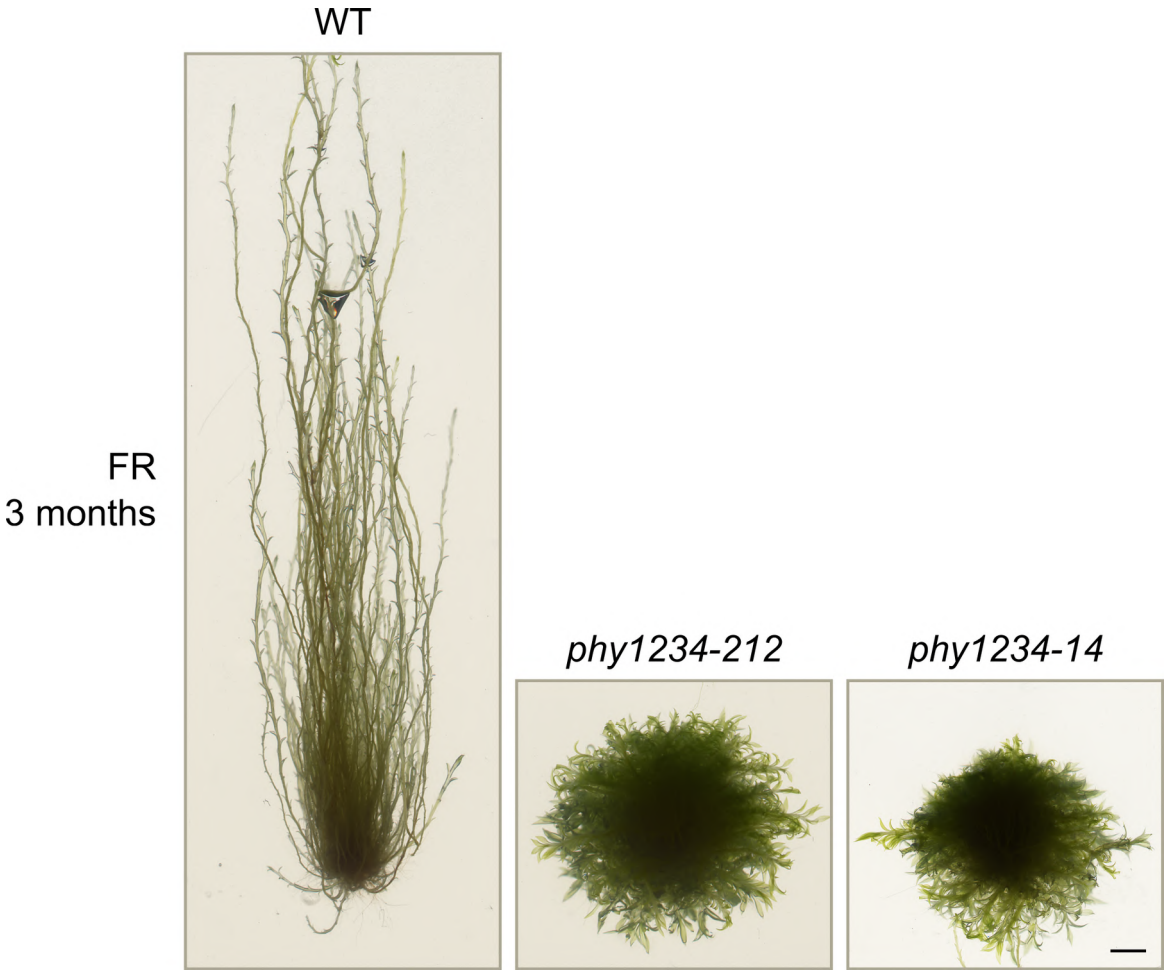

Fig. S17 Gametophore growth of WT and *phy1234* mutant plants in far-red light. Protonema of WT and two independent *phy1234* mutant lines was grown in standard growth conditions (white light, 50 µmol m^{-2} s^{-1}) on medium supplemented with 0.5 % sucrose for 10 days to induce gametophores and then transferred to far-red light (FR, 20 µmol m^{-2} s^{-1}) for 3 months. Plates were incubated vertically. Scale bar = 2 mm.

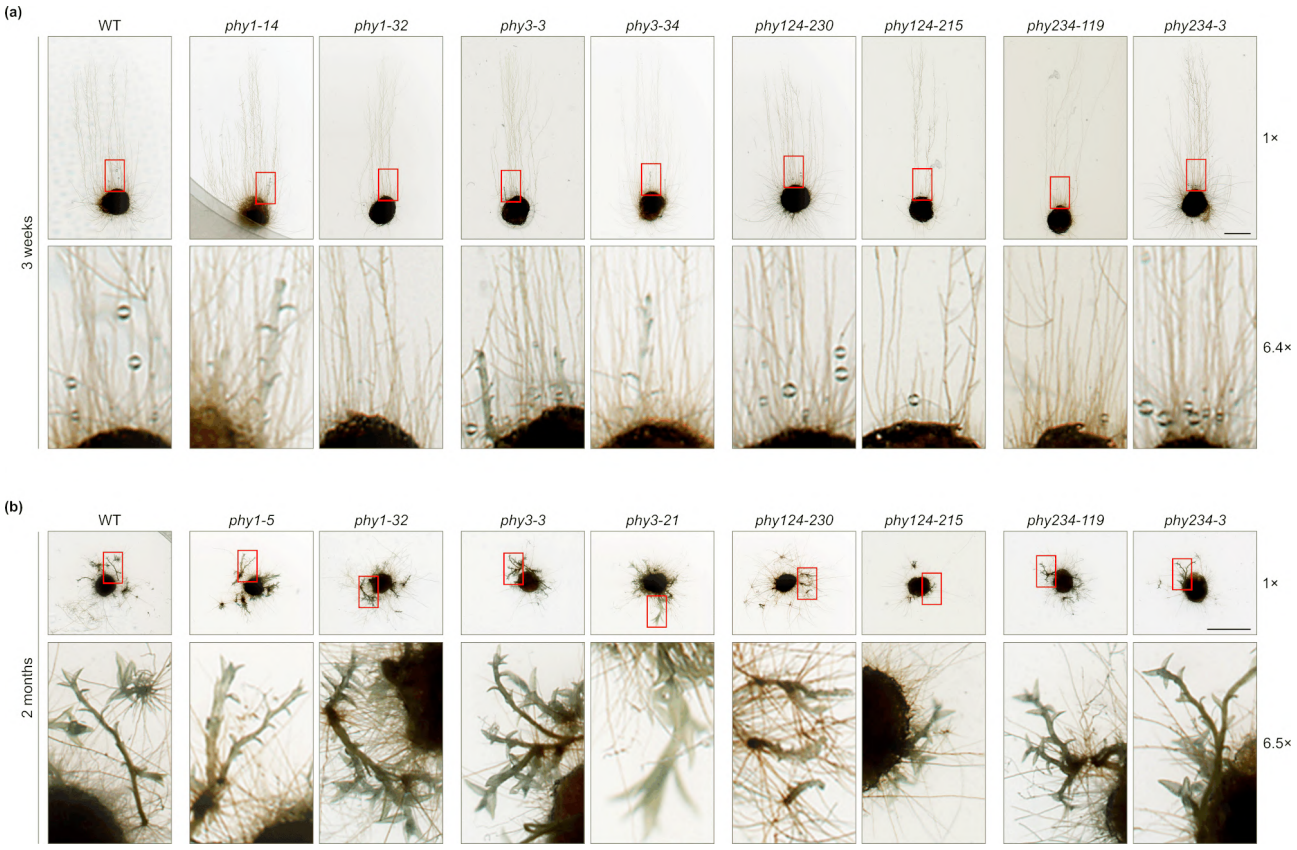

Fig. S18 PHY1 and PHY3 induce gametophores in far-red light. (a), (b) Freshly fragmented protonema cultures of WT, *phy1*, *phy3*, *phy124*, and *phy234* plants (two independent lines for each mutant) were grown (a) for 3 weeks (plates were incubated vertically) or (b) for 2 months in far-red light (20 µmol m^{-2} s^{-1}) on medium supplemented with 0.5 % sucrose. Scale bar = 2 mm in (a) and 5 mm in (b). Red squares indicate magnified areas; magnification is shown on the right of the respective pictures.

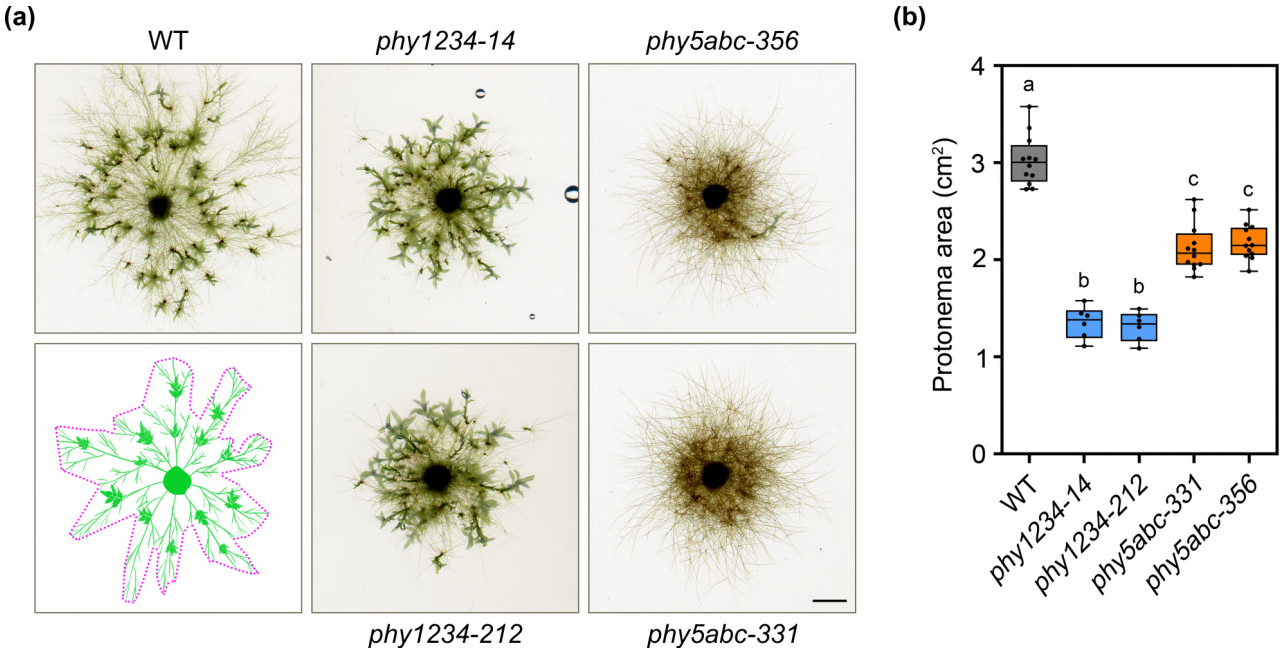

Fig. S19 *phy1234* and *phy5abc* grown in blue light. Protonema cultures of WT, *phy1234*, and *phy5abc* plants (two independent lines for each mutant) were grown for 45 days in blue light (B, 12 µmol m^{-2} s^{-1}) on solid Knop's medium supplemented with 0.5 % sucrose. Scale bar = 2 mm. The picture on the left, lower row shows how protonema area (indicated by the purple dotted line) was quantified. (b) Protonema area was measured as shown in (a). Data are shown as box plot (number of plants ≥ 6); different letters indicate significant differences as determined by one-way ANOVA followed by post-hoc Tukey's HSD test; $p < 0.05$.

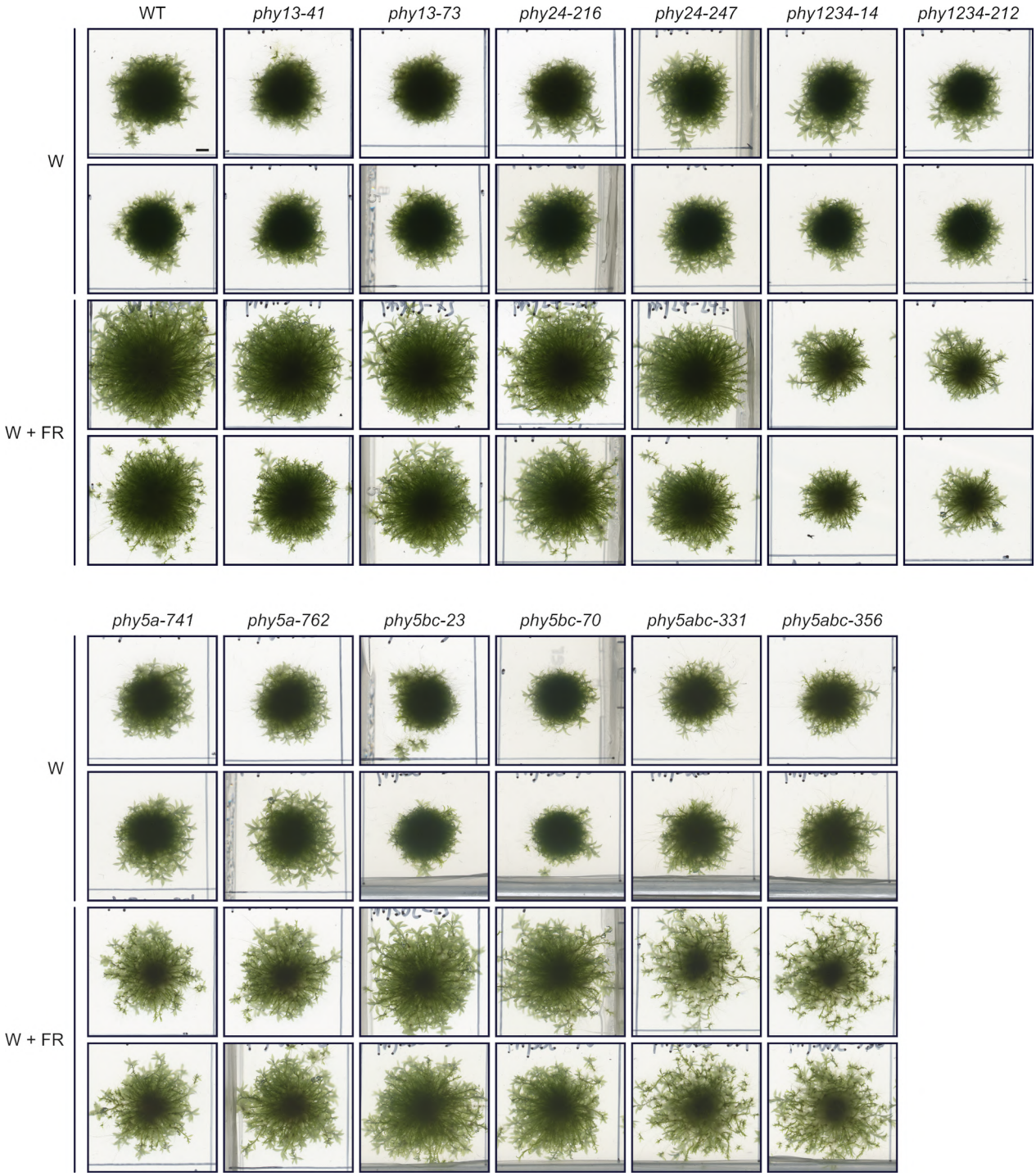

Fig. S20 Enhanced gametophore growth in low R:FR light is impaired in *phy1234*. WT and two independent lines for each mutant were grown in high R:FR conditions (white light without supplemental far-red light, W, 25 µmol m^{-2} s^{-1}) or low R:FR conditions (white light supplemented with far-red light, W + FR; both 25 µmol m^{-2} s^{-1}) for 45 days. Two plants are shown for each line/light condition. Scale bar = 2 mm.

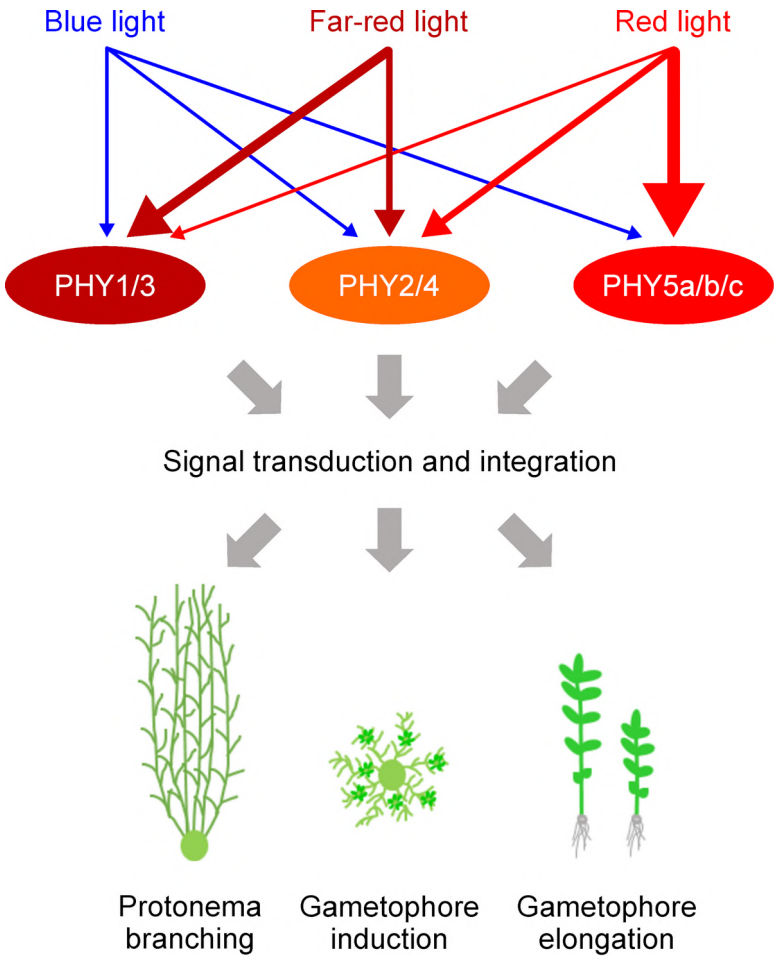

Fig. S21 *Physcomitrium* phytochromes respond to diverse light conditions and play specific and overlapping roles in sensing different light qualities. The thickness of the red, far-red and blue arrows indicates to which extent the different phytochromes contribute to responses induced by the respective light condition. See text for details.

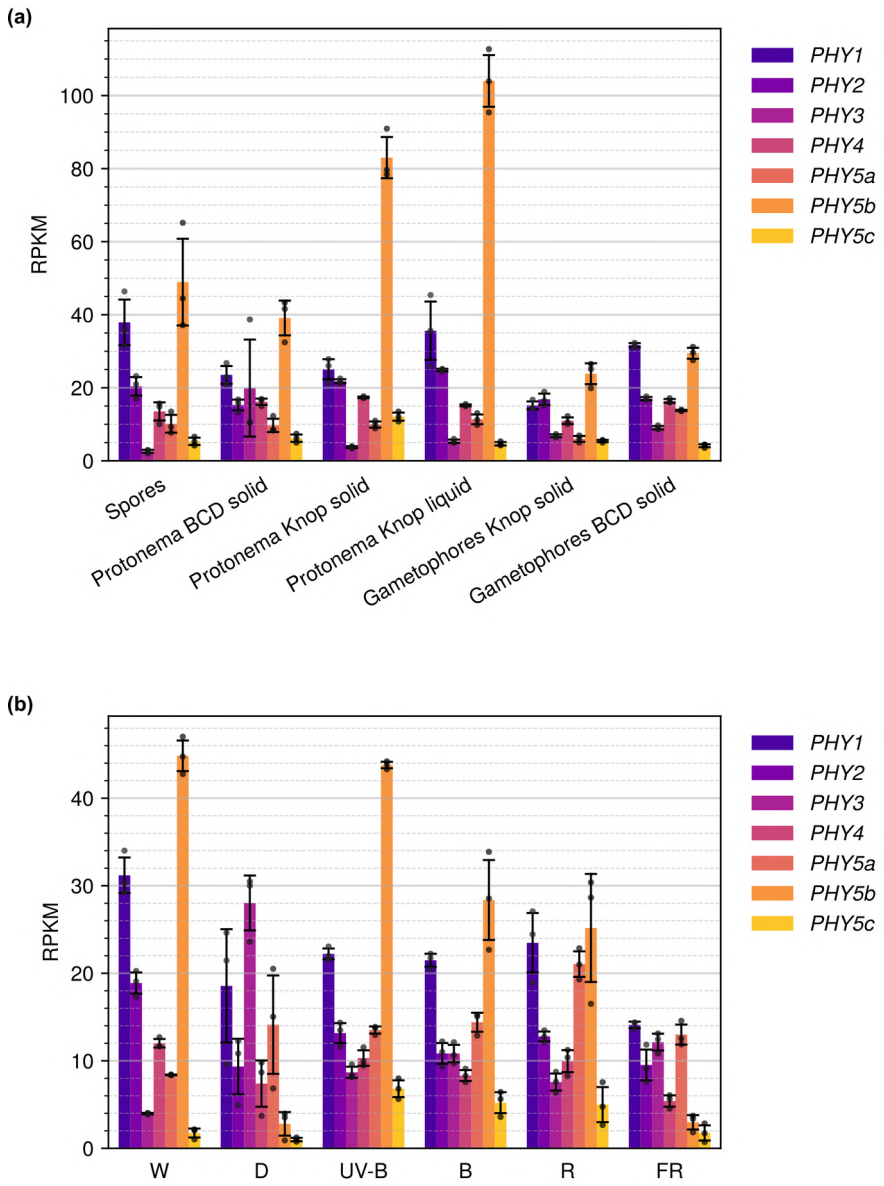

Fig. S22 Tissue-specificity and light-regulation of expression of *Physcomitrium* phytochromes. (a), (b) Summary of RNA-seq data from Perroud *et al.* (2018) provided through PEATmoss (Fernandez-Pozo *et al.*, 2020). (a) Expression of *Physcomitrium* phytochromes in different tissues (spores, protonema, gametophores) on different substrates (solid BCD medium, solid or liquid Knop medium). (b) Expression of *Physcomitrium* phytochromes in protonema exposed to different light conditions (W, continuous white light; D, dark; UV-B, continuous white light supplemented with UV-B; B, continuous blue light; R, continuous red light; FR, continuous far-red light). (a), (b) For detailed experimental procedures and light sources, refer to Peroud *et al.* (2018). Bars show mean RPKM of three replicates ± SD.

Table S1 gBlock fragments containing the U6 promoter (blue) and coding for the respective sgRNAs (crRNA, red, bold; tracRNA, orange, underlined). The U6-sgRNA cassette is flanked by *attB1*/*attB2* sites (magenta, lower case). Lower case in the sequence coding for the crRNA indicates nucleotides that have been changed to G to be in line with the recommendations in Ermert *et al.* (2019).

Name	gBlock sequence
U6-PHY1-sgRNA	ggggacaagtttgtacaaaaaagcaggcttcGTCCATTGAAGCAGACGTGTTGCGA CAGGTTAGCGACGATGGGTGTAGATGTGATGTGATGTGATGGTGTGGTTCTTCCAC GGCGGCGTCCTTGCGGTGGCGGAGAAGGGGATATCCCGAAGGAGCGGCAGCGGGAG AGCACAAGCAGAAAGGGTGCAGTGAGTGAGTGGGTCCAGCTGGGTGGCTGGCCGAG TGGACGCGACCGGGTTTCGAGGGGGcGGGGGAGAAAAGGGATGGAGCGAGGGATAT AACCCACATGGAATGGAGGTGGGTGTGAAGGCGGGTATATAGGAAGGTGGAGGACT TACAACCCAT**gGTGGCTGAGATACGTCGCG**GTTTTAGAGCTAGAAATAGCAAGTTA AAATAAGGCTAGTCCGTTATCAACTTGAAAAAGTGGCACCGAGTCGGTGCTTTTTT TGAGCTCGTCgacccagctttcttgtacaaagtggtcccc
U6-PHY2-sgRNA	ggggacaagtttgtacaaaaaagcaggcttcGTCCATTGAAGCAGACGTGTTGCGA CAGGTTAGCGACGATGGGTGTAGATGTGATGTGATGTGATGGTGTGGTTCTTCCAC GGCGGCGTCCTTGCGGTGGCGGAGAAGGGGATATCCCGAAGGAGCGGCAGCGGGAG AGCACAAGCAGAAAGGGTGCAGTGAGTGAGTGGGTCCAGCTGGGTGGCTGGCCGAG TGGACGCGACCGGGTTTCGAGGGGGcGGGGGAGAAAAGGGATGGAGCGAGGGATAT AACCCACATGGAATGGAGGTGGGTGTGAAGGCGGGTATATAGGAAGGTGGAGGACT TACAACCCAT**gCTACATTACGCGCTCCTCA**GTTTTAGAGCTAGAAATAGCAAGTTA AAATAAGGCTAGTCCGTTATCAACTTGAAAAAGTGGCACCGAGTCGGTGCTTTTTT TGAGCTCGTCgacccagctttcttgtacaaagtggtcccc
U6-PHY3-sgRNA	ggggacaagtttgtacaaaaaagcaggcttcGTCCATTGAAGCAGACGTGTTGCGA CAGGTTAGCGACGATGGGTGTAGATGTGATGTGATGTGATGGTGTGGTTCTTCCAC GGCGGCGTCCTTGCGGTGGCGGAGAAGGGGATATCCCGAAGGAGCGGCAGCGGGAG AGCACAAGCAGAAAGGGTGCAGTGAGTGAGTGGGTCCAGCTGGGTGGCTGGCCGAG TGGACGCGACCGGGTTTCGAGGGGGcGGGGGAGAAAAGGGATGGAGCGAGGGATAT AACCCACATGGAATGGAGGTGGGTGTGAAGGCGGGTATATAGGAAGGTGGAGGACT TACAACCCAT**gGTCCGCACCAAAAATAGGA**GTTTTAGAGCTAGAAATAGCAAGTTA AAATAAGGCTAGTCCGTTATCAACTTGAAAAAGTGGCACCGAGTCGGTGCTTTTTT TGAGCTCGTCgacccagctttcttgtacaaagtggtcccc
U6-PHY4-sgRNA	ggggacaagtttgtacaaaaaagcaggcttcGTCCATTGAAGCAGACGTGTTGCGA CAGGTTAGCGACGATGGGTGTAGATGTGATGTGATGTGATGGTGTGGTTCTTCCAC GGCGGCGTCCTTGCGGTGGCGGAGAAGGGGATATCCCGAAGGAGCGGCAGCGGGAG AGCACAAGCAGAAAGGGTGCAGTGAGTGAGTGGGTCCAGCTGGGTGGCTGGCCGAG TGGACGCGACCGGGTTTCGAGGGGGcGGGGGAGAAAAGGGATGGAGCGAGGGATAT AACCCACATGGAATGGAGGTGGGTGTGAAGGCGGGTATATAGGAAGGTGGAGGACT TACAACCCAT**GCTTGACCTGATGCCACAAG**GTTTTAGAGCTAGAAATAGCAAGTTA AAATAAGGCTAGTCCGTTATCAACTTGAAAAAGTGGCACCGAGTCGGTGCTTTTTT TGAGCTCGTCgacccagctttcttgtacaaagtggtcccc
U6-PHY5a-	ggggacaagtttgtacaaaaaagcaggcttcGTCCATTGAAGCAGACGTGTTGCGA

sgRNA	CAGGTTAGCGACGATGGGTGTAGATGTGATGTGATGTGATGGTGTGGTTCTTCCAC GGCGGCGTCCTTGCGGTGGCGGAGAAGGGGATATCCCGAAGGAGCGGCAGCGGGAG AGCACAAGCAGAAAGGGTGCAGTGAGTGAGTGGGTCCAGCTGGGTGGCTGGCCGAG TGGACGCGACCGGGTTTCGAGGGGGcGGGGGAGAAAAGGGATGGAGCGAGGGATAT AACCCACATGGAATGGAGGTGGGTGTGAAGGCGGGTATATAGGAAGGTGGAGGACT TACAACCCAT**GCTTACGGCTAACAAGAGAA**GTTTTAGAGCTAGAAATAGCAAGTTA AAATAAGGCTAGTCCGTTATCAACTTGAAAAAGTGGCACCGAGTCGGTGCTTTTTT TGAGCTCGTCgacccagctttcttgtacaaagtggtcccc
U6-PHY5b-sgRNA	ggggacaagtttgtacaaaaaagcaggcttcGTCCATTGAAGCAGACGTGTTGCGA CAGGTTAGCGACGATGGGTGTAGATGTGATGTGATGTGATGGTGTGGTTCTTCCAC GGCGGCGTCCTTGCGGTGGCGGAGAAGGGGATATCCCGAAGGAGCGGCAGCGGGAG AGCACAAGCAGAAAGGGTGCAGTGAGTGAGTGGGTCCAGCTGGGTGGCTGGCCGAG TGGACGCGACCGGGTTTCGAGGGGGcGGGGGAGAAAAGGGATGGAGCGAGGGATAT AACCCACATGGAATGGAGGTGGGTGTGAAGGCGGGTATATAGGAAGGTGGAGGACT TACAACCCAT**gCGGAATCGGAACCGATGCG**GTTTTAGAGCTAGAAATAGCAAGTTA AAATAAGGCTAGTCCGTTATCAACTTGAAAAAGTGGCACCGAGTCGGTGCTTTTTT TGAGCTCGTCgacccagctttcttgtacaaagtggtcccc
U6-PHY5c-sgRNA	ggggacaagtttgtacaaaaaagcaggcttcGTCCATTGAAGCAGACGTGTTGCGA CAGGTTAGCGACGATGGGTGTAGATGTGATGTGATGTGATGGTGTGGTTCTTCCAC GGCGGCGTCCTTGCGGTGGCGGAGAAGGGGATATCCCGAAGGAGCGGCAGCGGGAG AGCACAAGCAGAAAGGGTGCAGTGAGTGAGTGGGTCCAGCTGGGTGGCTGGCCGAG TGGACGCGACCGGGTTTCGAGGGGGcGGGGGAGAAAAGGGATGGAGCGAGGGATAT AACCCACATGGAATGGAGGTGGGTGTGAAGGCGGGTATATAGGAAGGTGGAGGACT TACAACCCAT**GGAAAACGATGATTCATGCG**GTTTTAGAGCTAGAAATAGCAAGTTA AAATAAGGCTAGTCCGTTATCAACTTGAAAAAGTGGCACCGAGTCGGTGCTTTTTT TGAGCTCGTCgacccagctttcttgtacaaagtggtcccc

Table S2 Cloning of plasmid constructs and references to plasmids used in this study.

Name	Insert	Vector	Cloning strategy
pEntPp-U6-PHY1-sgRNA-KanR	U6-PHY1-sgRNA	pDONR207-KanR	A fragment coding for the U6-PHY1-sgRNA sequence flanked by *attB1*/*attB2* sites was synthesised at IDT. The sequence TGT GGC TGA GAT ACG TCG CG corresponds to the *PHY1* gRNA. The pEntPp-U6-PHY1-sgRNA-KanR plasmid was obtained by recombining the U6-PHY1-sgRNA fragment into pDONR207-KanR by BP Gateway cloning.
pEntPp-U6-PHY2-sgRNA-KanR	U6-PHY2-sgRNA	pDONR207-KanR	A fragment coding for the U6-PHY2-sgRNA sequence flanked by *attB1*/*attB2* sites was synthesised at IDT. The sequence TCT ACA TTA CGC GCT CCT CA corresponds to the *PHY2* gRNA. The pEntPp-U6-PHY2-sgRNA-KanR plasmid was obtained by recombining the U6-PHY2-sgRNA fragment into pDONR207-KanR by BP Gateway cloning.
pEntPp-U6-PHY3-sgRNA-KanR	U6-PHY3-sgRNA	pDONR207-KanR	A fragment coding for the U6-PHY3-sgRNA sequence flanked by *attB1*/*attB2* sites was synthesised at IDT. The sequence CGT CCG CAC CAA AAA TAG GA corresponds to the *PHY3* gRNA. The pEntPp-U6-PHY3-sgRNA-KanR plasmid was obtained by recombining the U6-PHY3-sgRNA fragment into pDONR207-KanR by BP Gateway cloning.
pEntPp-U6-PHY4-sgRNA-KanR	U6-PHY4-sgRNA	pDONR207-KanR	A fragment coding for the U6-PHY4-sgRNA sequence flanked by *attB1*/*attB2* sites was synthesised at IDT. The sequence GCT TGA CCT GAT GCC ACA AG corresponds to the *PHY4* gRNA. The pEntPp-U6-PHY4-sgRNA-KanR plasmid was obtained by recombining the U6-PHY4-sgRNA fragment into pDONR207-KanR by BP Gateway cloning.
pEntPp-U6-PHY5a-sgRNA-KanR	U6-PHY5a-sgRNA	pDONR207-KanR	A fragment coding for the U6-PHY5a-sgRNA sequence flanked by *attB1*/*attB2* sites was synthesised at IDT. The sequence GCT TAC GGC TAA CAA GAG AA corresponds to the *PHY5a* gRNA. The pEntPp-U6-PHY5a-sgRNA-KanR plasmid was obtained by recombining the U6-PHY5a-sgRNA fragment into pDONR207-KanR by BP Gateway cloning.

pEntPp-U6-PHY5b-sgRNA-KanR	U6-PHY5b-sgRNA	pDONR207-KanR	A fragment coding for the U6-PHY5b-sgRNA sequence flanked by *attB1*/*attB2* sites was synthesised at IDT. The sequence TCG GAA TCG GAA CCG ATG CG corresponds to the *PHY5b* gRNA. The pEntPp-U6-PHY5b-sgRNA-KanR plasmid was obtained by recombining the U6-PHY5b-sgRNA fragment into pDONR207-KanR by BP Gateway cloning.
pEntPp-U6-PHY5c-sgRNA-KanR	U6-PHY5c-sgRNA	pDONR207-KanR	A fragment coding for the U6-PHY5c-sgRNA sequence flanked by *attB1*/*attB2* sites was synthesised at IDT. The sequence GGA AAA CGA TGA TTC ATG CG corresponds to the *PHY5c* gRNA. The pEntPp-U6-PHY5c-sgRNA-KanR plasmid was obtained by recombining the U6-PHY5c-sgRNA fragment into pDONR207-KanR by BP Gateway cloning.
pDONR207-KanR			Lopez-Obando *et al.* (2016)
pAct-Cas9	pActin-Cas9		Lopez-Obando *et al.* (2016)

Table S3 Primers used for characterisation of *phy* mutant lines by PCR and sequencing.

Name	Primer sequence	Description
jh056-F	ACACGGCTTCAAGCATTACC	*PHY1*; PCR and sequencing
jh057-R	GCAATTATCCGCACCTTGTT	*PHY1*; PCR and sequencing
jh058-F	GGGCTTACATTACCCAGCAA	*PHY2*; PCR and sequencing
jh059-R	CATATACTGCGCATGGCAAC	*PHY2*; PCR and sequencing
jh089-F	GCGTTTGTTTTGTTGGTCAGG	*PHY3*; PCR and sequencing
jh090-R	TCACTTCATCTCGCTTCCAACC	*PHY3*; PCR and sequencing
jh062-F	AATCCACTGGCGAGAATGTC	*PHY4*; PCR and sequencing
jh063-R	AACTTCCTGCTGACCCACAC	*PHY4*; PCR and sequencing
jh081-F	CTTGGAAAAATGCTGGTTGG	*PHY5a*; PCR and sequencing
jh082-R	GCAATGTGCAGAAAGCAAAA	*PHY5a*; PCR and sequencing
jh083-F	GGTCATTGCATACAGTGAGA	*PHY5b*; PCR and sequencing
jh084-R	CGTAAAATGGCTTCCCTGAA	*PHY5b*; PCR and sequencing
jh085-F	AATGGATGCGATCCACTCTC	*PHY5c*; PCR and sequencing
jh086-R	CTTGAGTCCACCGCAAGAAT	*PHY5c*; PCR and sequencing

Table S4 Accession numbers of genes/proteins used in this study.

Gene/ protein	Species	Database	Accession number
PHY1	*Physcomitrium patens*	Phytozome (https://phytozome.jgi.doe.gov/)	Pp3c25_2610
PHY2	*Physcomitrium patens*	Phytozome (https://phytozome.jgi.doe.gov/)	Pp3c16_20280
PHY3	*Physcomitrium patens*	Phytozome (https://phytozome.jgi.doe.gov/)	Pp3c16_18760
PHY4	*Physcomitrium patens*	Phytozome (https://phytozome.jgi.doe.gov/)	Pp3c27_7830
PHY5a	*Physcomitrium patens*	Phytozome (https://phytozome.jgi.doe.gov/)	Pp3c3_23790
PHY5b	*Physcomitrium patens*	Phytozome (https://phytozome.jgi.doe.gov/)	Pp3c12_9240
PHY5c	*Physcomitrium patens*	Phytozome (https://phytozome.jgi.doe.gov/)	Pp3c4_15350
phyA	*Arabidopsis thaliana*	UniProt (https://www.uniprot.org/)	P14712
phyB	*Arabidopsis thaliana*	UniProt (https://www.uniprot.org/)	P14713

REFERENCES

Carpenter EJ, Matasci N, Ayyampalayam S, Wu S, Sun J, Yu J, Jimenez Vieira FR, Bowler C, Dorrell RG, Gitzendanner MA, *et al.* 2019. Access to RNA-sequencing data from 1,173 plant species: The 1000 Plant transcriptomes initiative (1KP). *GigaScience* **8**: giz126.

Ermert AL, Nogué F, Stahl F, Gans T, Hughes J. **2019**. CRISPR/Cas9-mediated knockout of *Physcomitrella patens* phytochromes. *Methods in Molecular Biology (Clifton, N.J.)* **2026**: 237–263.

Fernandez-Pozo N, Haas FB, Meyberg R, Ullrich KK, Hiss M, Perroud P-F, Hanke S, Kratz V, Powell AF, Vesty EF, *et al.* 2020. PEATmoss (Physcomitrella Expression Atlas Tool): a unified gene expression atlas for the model plant *Physcomitrella patens*. *Plant Journal* **102**: 165–177.

Lopez-Obando M, Hoffmann B, Géry C, Guyon-Debast A, Téoulé E, Rameau C, Bonhomme S, Nogué F. **2016**. Simple and efficient targeting of multiple genes through CRISPR-Cas9 in *Physcomitrella patens*. *Genes, Genomes, Genetics* **6**: 3647–3653.

NCBI Resource Coordinators. **2013**. Database resources of the National Center for Biotechnology Information. *Nucleic Acids Research* **41**: D8–D20.

Perroud P-F, Haas FB, Hiss M, Ullrich KK, Alboresi A, Amirebrahimi M, Barry K, Bassi R, Bonhomme S, Chen H, *et al.* 2018. The *Physcomitrella patens* gene atlas project: large-scale RNA-seq based expression data. *Plant Journal* **95**: 168–182.

Possart A, Hiltbrunner A. **2013**. An evolutionarily conserved signaling mechanism mediates far-red light responses in land plants. *Plant Cell* **25**: 102–114.